High-Cycle Fatigue Design Curves of Mild- and High-Strength Steels for Offshore Applications

High-Cycle Fatigue Design Curves of Mild- and High-Strength Steels for Offshore Applications

Paulo Mendes[1,*], José A.F.O Correia[1], António Mourão[1], Rita Dantas[1,2], Abílio de Jesus[2,3], Claúdio Horas[1], Nicholas Fantuzzi[4], Lance Manuel[5]

Abstract

Fatigue analysis holds profound significance in the design and maintenance of offshore wind energy systems, especially within the framework for transitioning from oil and gas to renewable energies. Addressing the impact of fatigue life variability is essential when generating reliable S-N curves and establishing safe operational domains. In contrast to commonly applied global S-N approaches presented in standards, local approaches provide a more comprehensive understanding of the material's fatigue strength. This study implements various probabilistic methods for generating fatigue strength curves, including the guidelines recommended by ISO 12107, a two-parameter Weibull distribution, the Castillo & Fernández-Canteli (CFC) model, and a Bayesian method that incorporates a Markov Chain Monte Carlo algorithm. Using experimental data from literature for S355 (base) and S690QL (base and welded) steels, two distinct model fitting approaches - classical linear regres-

*pjmendes@fe.up.pt

[1]CONSTRUCT-LESE, Faculty of Engineering, University of Porto, Porto, Portugal

[2]INEGI - Instituto de Ciência e Inovação em Engenharia Mecânica e Engenharia Industrial, Porto, Portugal

[3]Faculty of Engineering, University of Porto, Portugal

[4]University of Bologna, Bologna, Italy

[5]University of Texas, Austin, USA

sion (CLR) and orthogonal linear regression (OLR) - were applied. Also, this study explores how corrosion affects fatigue strength by deriving fatigue strength curves that consider this influence. In practical scenarios, CLR is recommended for the design of new projects, whereas OLR is recommended for retrofitting purposes in order to leverage the structural capacity and fatigue resistance of materials and structures that have been in long-term operation. Based on this comparative analysis, the most conservative model for CLR is the two-parameter Weibull distribution, whereas the most conservative model for OLR is the Bayesian approach incorporating the Markov Chain Monte Carlo algorithm. These models are identified as particularly well-suited for high-cycle fatigue, predicting shorter fatigue lives and indicating a higher potential for fatigue damage, thereby enhancing fatigue strength modelling for current offshore materials.

Keywords: Fatigue design, S355 steel, S690QL steel, Offshore structures, Probabilistic modelling, Statistical analysis, Corrosion

---

1. Introduction

The transition to renewable energy is a global imperative, and offshore structures have emerged as key players in this transformation [1–6]. As the offshore wind industry grows, it is important to determine safe and sustainable methods for disposing, using, or repurposing these existing structures. [7–11]. The vast majority of offshore structures, specially fixed offshore platforms, have been constructed using medium-grade structural steels with yield strengths around 355 MPa. The use of high-strength steels, characterised by yield strengths above 420 MPa, is increasingly gaining prominence in the offshore industry, since their superior performance enhances the strength-to-

weight ratio, reduces costs, shortens construction timelines [12], and improves fatigue resistance. Fatigue is a complex phenomenon that can lead to the failure of mechanical components and materials, being defined as the progressive degradation resultant of repeated stress-strain cycles, leading to gradual cracking and eventual fracture. This intricate phenomenon is responsible for approximately half of all mechanical failures [13]. In the context of welded joints, fatigue failure can be initiated by regions of stress concentration [14–19]. Cui [20] highlighted recent developments in fatigue life prediction methods, categorising influencing factors, including material properties, structure, applied loads, and environmental conditions.

The fatigue life of a structure depends on stochastic variables that cannot be predicted with certainty, relying instead on a certain degree of probability. Therefore, a fatigue design criteria should consider probabilistic modelling and analysis, accounting for the variability in applied loads, material strength and structural details [21–23]. The intrinsic nature of uncertainty in input data is demonstrated by its scatter, often quantified by the coefficient of variation (CV) [24]. This statistical parameter, expressed as the ratio of the standard deviation (σ_x) to the mean value (μ_x) of the parameter or random variable x, is denoted as $CV_x = \frac{\sigma_x}{\mu_x}$. Some parameters such as the conventional fatigue endurance limit, σ_0, and the fatigue strength coefficient, σ'_f, present some degree of uncertainty associated. According with some authors [24–26], the coefficient of variation of σ_0 ranges between 0.05 and 0.1 for plain specimens and between 0.1-0.2 for welded joints. Additionally, for the σ'_f the CV is assumed as 0.05, as suggested in [24–26]. Thus, adopting a probabilistic modelling approach is essential to integrate the inherent

uncertainty in input data into fatigue-life assessment.

Conventional S-N or Wohler's curves, which provide deterministic average life predictions, fall short in designing for applications that must account for variability. Therefore, using stochastic methods to elaborate probabilistic S-N fields (p-S-N fields) offers reliable estimates for structural design, considering the inherent uncertainty in fatigue life [27–35]. Many probabilistic distributions have been proposed for the prediction of fatigue life [8, 23, 34–40], and to gain valuable insights into the fatigue behaviour of materials and structural details.

Correia et al. [41] proposed an unified approach for deriving probabilistic S–N fields for notched details, considering both crack initiation and crack propagation phases, based on experimental data and numerical simulation. Strzelecki et al. [42] introduced an innovative analytical method for deriving the S-N curve characteristics of aluminum material. Kang et al. [43] presented a probabilistic fatigue reliability assessment method for steel members using Gumbel, lognormal, exponential, and Weibull probability distributions. Caiza et al. [44] suggested S-N curves based on the Stüssi model and the Weibull distribution function to strength the modelling of structural details. In a recent study, Correia et al. [45] developed a fatigue strength assessment methodology for riveted railway bridge details based on regression analyses combined with probabilistic models. Other authors [46, 47] have established design S-N curves using a Bayesian approach, which has proven its capability to offer more accurate estimates of the fatigue strength of materials and structural components compared to classical statistical methods.

Corrosion stands out as a primary structural degradation process that

significantly impacts structural integrity, a reduction in the effective cross-sectional area, moment of inertia, torsional and warping constants [48, 49]. The interaction between corrosion and cyclic loading, commonly recognised as corrosion fatigue, affects the mechanical properties of steel, resulting in the initiation of cracks from the corrosion-induced surface and a substantial decrease in fatigue strength [50–53]. This degradation is evident in a typical S-N curve of a material exposed to an air environment influenced by the corrosion process, as depicted in Figure 1.

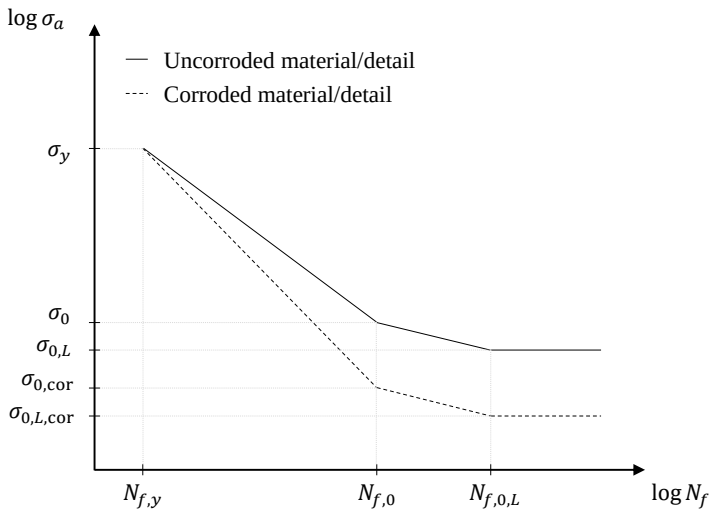

Figure 1: Effect of corrosion on the S-N curve of materials or details, adapted from [53].

The stress-based approach stands as the preferred method for predicting crack initiation in structural components/materials subject to load-controlled conditions and to describe the medium and high-cycle fatigue regime. This approach is particularly effective when stress levels predominantly fall within the elastic range of the material, minimising plastic deformation and non-linear behaviour [34, 54]. Among local approaches, the stress-based approach

one, which utilises the applied stress amplitude, σ_a, to predict the number of cycles to failure, N_f, is the most commonly used due to its ease of application and the abundance of literature on the fatigue properties of materials. The stress-based approach, expressed through the Basquin law [55], is given by Equation 1:

$$\sigma_a = \sigma'_f (N_f)^b \tag{1}$$

where, σ_a represents the stress amplitude, σ'_f represents the fatigue strength coefficient, b is the fatigue strength exponent commonly between $-0.12 < b < -0.05$ with an average of -0.085 [24], and N_f is the number of cycles until failure.

Based on the same stress-based approach, a formula for the S-N curve of corroded steel was proposed by Adasooriya et al. [52]. This concept is based on the degradation mechanism (corrosion effects) discussed in [52, 53] and is expressed in Equation 2:

$$\sigma_{a,\text{cor}} = \left(\sigma'_f N_{f,y}^c\right) N_f^{(b-c)}, \text{ with } c = \log\left[\frac{\sigma_0}{\sigma_{0,\text{cor}}}\right] / \log\left[\frac{N_{f,0}}{N_{f,y}}\right] \tag{2}$$

where, $\sigma_{a,\text{cor}}$ represents the fatigue strength of corroded material corresponding to the number of cycles until failure, N_f, and $\sigma_{0,\text{cor}}$ represents the constant amplitude fatigue limit for the corroded material. The constant amplitude fatigue limit represents the maximum stress that a structural element or material can withstand under constant amplitude loading without experiencing fatigue failure over a specific number of cycles. These limits are defined for specific numbers of cycles to failure, with $N_{f,0}$ set as 5E6 cycles for the Eurocode 3: Part 1-9 [56], and 1E7 cycles for the DNVGL-RP-C203 [57]

standard, respectively. These authors [53] postulated that when the stress amplitude is equal to the yield strength, σ_y, the number of cycles to fatigue failure of the uncorroded material is denoted as $N_{f,y}$ and is dependent on the yield strength and on the high-cycle fatigue curve for the uncorroded material.

When conducting fatigue tests under different stress ratios, it is necessary to consider the influence of mean stress. To address this influence, a mean stress adjustment can be applied to convert a stress cycle into an equivalent stress cycle without the mean stress influence. Several approaches have been proposed to address the impact of mean stress on fatigue life for steels and alloys, including the Soderberg, Goodman, and Gerber diagrams [58–60]. Dowling et al. [61] provides a comparative analysis of different methods to account for mean stress in fatigue analysis, highlighting the limitations and strengths of each method, and noting material-specific considerations for steels and aluminium alloys. For steels, the Walker method [62] produces better outcomes when there is data accessible for adjusting the parameter γ. Equation 3 provides a relationship between the stress ratio, stress amplitude and the parameter γ in order to normalise the stress amplitude $\sigma_{a,\text{norm}}$ to completely reversed conditions ($R = -1$).

$$\sigma_{a,\text{norm}} = \sigma_a \left(\frac{2}{1-R} \right)^{1-\gamma} \tag{3}$$

The material property, γ, from Equation 3 can be estimated using Equation 4 which relates γ with the tensile strength, σ_u, of steels.

$$\gamma = -0.0002\sigma_u + 0.8818 \tag{4}$$

In this work, results obtained from fatigue testing conducted on S355 mild steel and S690QL base and welded steels were used for probabilistic fatigue characterization, considering their widespread application in the offshore industry. The proposed statistical methods were implemented to analyse the obtained experimental data and to establish reliable uncorroded and corroded fatigue curves. It is noteworthy that the derivation of the corroded fatigue curve was based on postulated fatigue data. The parameters for these fatigue curves were obtained using the classical linear (CLR) and orthogonal linear regression (OLR) methods. A conservative approach was adopted for both methods, with CLR being the preferred choice for novel project design, due to its simplicity and interpretability. On the other hand, when aiming to improve longevity, OLR was recommended. CLR allows for a straightforward understanding of fundamental relationships between variables, making it suitable for designing innovative fatigue-resistant systems. In contrast, OLR ensures the stability of parameter estimates over time, proving advantageous for this type of applications where model consistency is required throughout the entire lifespan of the system. The structure of this paper is organised in five sections: Section 2 provides details on the materials used in this study. Section 3 and 4 describe the proposed models behind this probabilistic modelling, presenting the resulting uncorroded and corroded probabilistic fatigue strength curves and conducting a comparative analysis. Conclusions, along with decisive findings, are presented in Section 5.

2. Materials and experimental details

Dantas et al. [63] evaluated the fatigue behaviour of the S355J2 structural steel material in the high-cycle fatigue regime. This work involved uniaxial and biaxial (axial+torsion in-phase) fatigue tests conducted under different stress ratios, with loads applied using sinusoidal functions of constant amplitude at a frequency of 10 Hz. For the sake of this work, only the axial fatigue results were taken into consideration.

Mendes et al. [64] performed fatigue tests with alternating tensile and compressive stresses on two distinct specimens- S690QL base steel material (BM) and S690QL welded steel material (WM). A total of 56 and 26 specimens were used for the S690QL base and welded steels, respectively, derived from a 30-millimeters (J30) and a 60-millimeters (J60) thick S690QL steel welded joints. The fatigue tests for the S690QL steel welded joints were conducted under rotating bending, with a stress ratio of $R = -1$, and performed at a frequency of 23 Hz.

Tables 1 and 2 present the mechanical properties and the chemical composition of the S355 and S690QL base and welded steels, as reported in [63] and [64], respectively. Coreweld 69 LT H4 is the metal cored wire used as weld steel for the welding of the S690QL plates [65]. These mechanical properties were supplied by the steel manufacturer, and therefore, they should include some level of uncertainty. In Table 2, the coefficients of variation, associated with each material, were based on default values suggested by P.H Wirsching [66].

Table 1: Chemical composition (wt.%) of the S355, S690QL base and welded steels.

Material	C	Si	Mn	P	S	Cr	Cu	Ni	Al	Mo	Ti	Nb, V, N, B
S355	0.160	0.300	1.280	0.030	0.002	0.200	0.200	-	-	-	-	0.009
S690QL (J30)	0.140	0.279	1.203	0.020	0.002	0.299	0.025	0.011	0.035	0.178	0.016	0.050
S690QL (J60)	0.149	0.276	1.253	0.011	0.001	0.621	0.030	0.012	0.030	0.259	0.016	0.023
Coreweld 69 LT H4	0.050	0.500	1.700	0.011	0.008	0.060	-	2.300	0.010	0.500	0.012	0.005

Table 2: Mechanical properties for the S355 and S690QL base and welded steels with associated uncertainty.

Material	**Yield strength,** σ_y **[MPa]**	CV, σ_y	**Tensile strength,** σ_u **[MPa]**	CV, σ_u
S355	367	0.07	579	0.05
S690QL (J30)	814	0.07	857	0.05
S690QL (J60)	758	0.07	835	0.05
Coreweld 69 LT H4	755	0.07	790	0.05

In Figure 2 a) and Figure 2 b), the experimental data points for the S355 base and for the S690QL base and welded steels are represented. Note that the experimental data points marked with an arrow ($\longrightarrow$) represent run-outs. For detailed experimental fatigue results from the testing conducted by Dantas et al. [63] and Mendes et al. [64], please refer to the data provided in Appendix A. As the experimental data for the S355 was obtained under different stress ratios, it was necessary to normalise stresses for the same stress ratio. For comparison purposes, Figure 3 depicts all the experimental fatigue data normalised to the stress amplitude under completely reversed conditions ($R = -1$) using Equation 3.

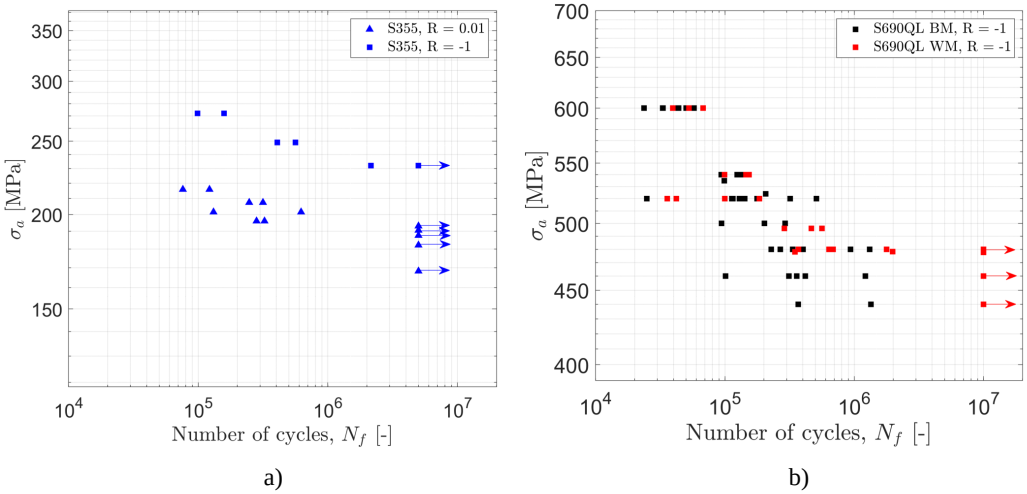

a) b)

Figure 2: Experimental fatigue data for the a) S355 [63] and b) S690QL base and welded steels [64].

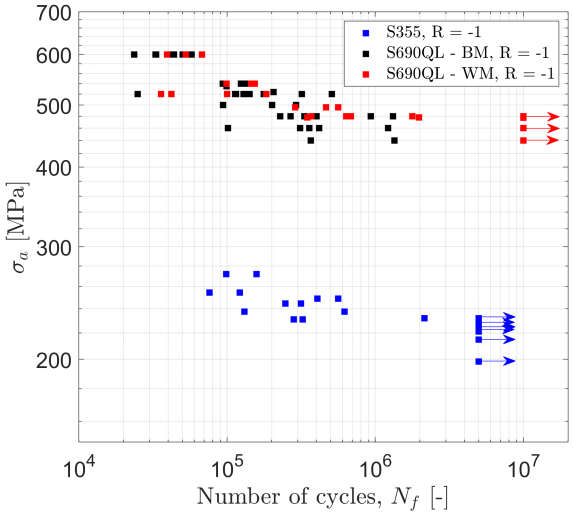

Figure 3: Experimental normalised fatigue data for S355 base [63] and S690QL base and welded steels [64].

3. Probabilistic fatigue strength modelling

3.1. Fitting methods - regression analysis

Different probability distributions and models were used to establish fatigue curves, relating σ_a and N_f, with a comparison being conducted between them. The flowchart presented in Figure 4 summarises the different steps taken in this work to analyse the experimental data and derive reliable fatigue strength curves.

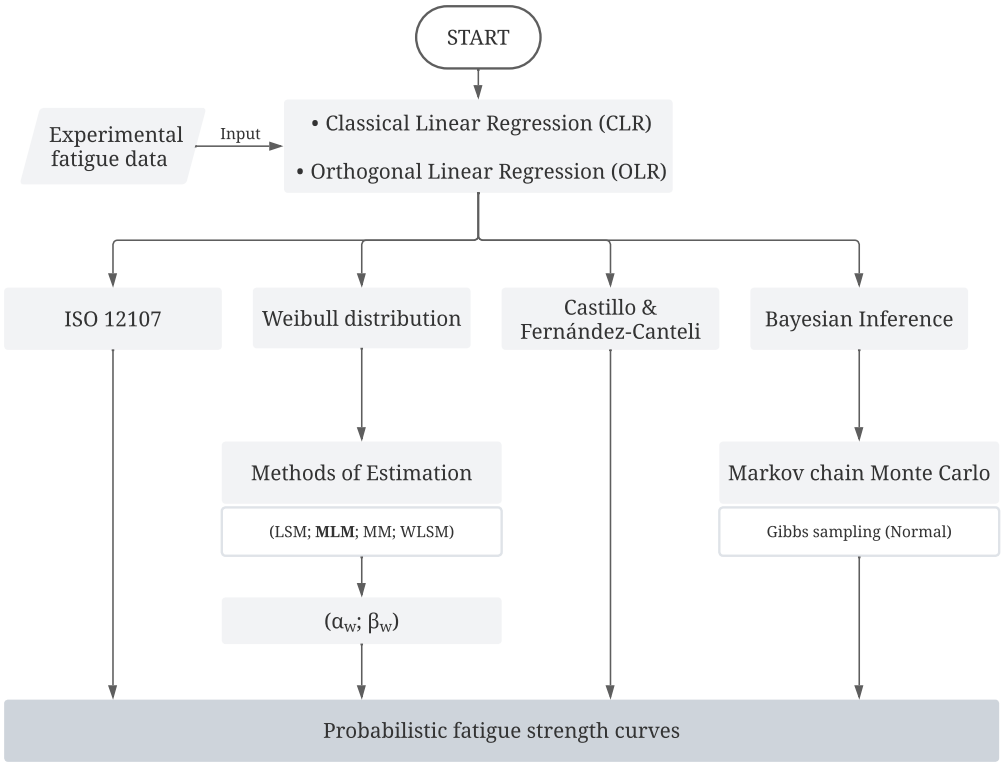

Figure 4: Flowchart describing the probabilistic modelling procedure to obtain reliable fatigue curves.

Classical linear regression (CLR) (Figure 5 a)), often referred to as ordi-

nary least squares (OLS) regression, is a method used to identify trends in data by fitting a straight line to the variables. In a graph with an X-axis and a Y-axis, usually X represents the independent variable (or predictor variable), while Y represents the dependent variable (or response variable). Classical linear regression introduces asymmetry between the variables and seeks to minimise the vertical distances in Y and horizontal distances in X.

Orthogonal linear regression (OLR) (Figure 5 b)), also known as total least squares (TLS) regression, is a method that symmetrically relates the variables X and Y, unlike classical linear regression. In this model, the minimised distances are the orthogonal distances (perpendicular distances) from the data points to the obtained regression-fitted line. This means that if the variables are inverted, the minimised distances will remain the same. OLR is particularly advantageous when the aim is to minimise errors in both the $X-$ and Y-directions, which is relevant when the data contains uncertainties in both variables. OLR tends to yield robust parameter estimates against variations in the data and errors and effectively handle outliers, which are examples of data discrepancies. This attribute contributes to enhanced reliability in predicting fatigue behaviour.

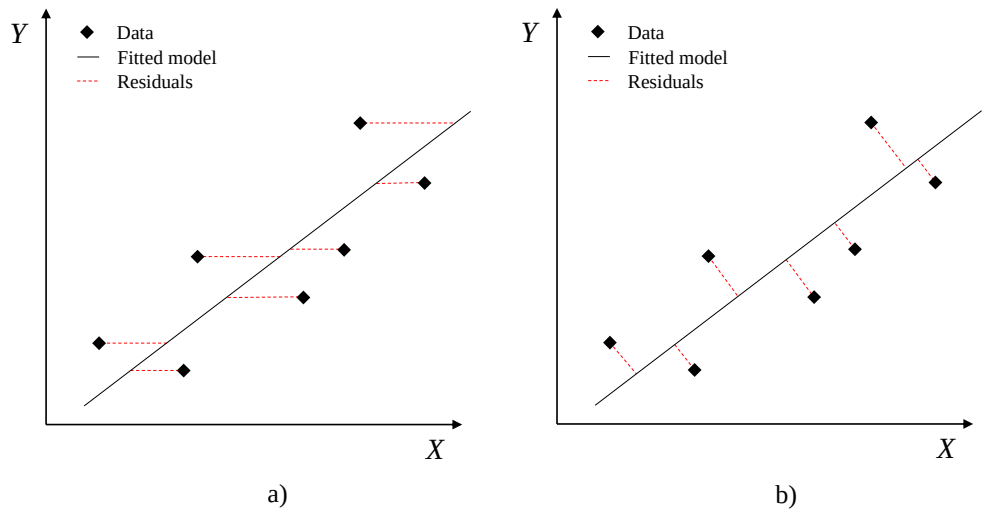

Figure 5: Linear regression methods: a) Classical linear regression (CLR); b) Orthogonal linear regression (OLR).

Estimating the parameters that define the linear relationship between the variables using linear regression is an important step. Assuming $\log N_f$ as the dependent variable and $\log \sigma_a$ as the independent variable (denoted as Y and X, respectively), the linear fit equation, Equation 5, is used:

$$\log N_f = A + B \log \sigma_a \quad \Leftrightarrow \quad Y = A + BX \tag{5}$$

The parameters, A and B, are the linear fit coefficients of the model, which are obtained by minimising the sum of squares of the residuals. This involves replacing the values in Equation 5 to obtain Equation 6:

$$\hat{A} = \bar{Y} - \hat{B}\bar{X} \tag{6}$$

where, $\hat{A}$ and $\hat{B}$ are the estimated constants, $\bar{X} = \frac{1}{n}\sum_{i=1}^{n} X_i$ and $\bar{Y} = \frac{1}{n}\sum_{i=1}^{n} Y_i$ are the mean values of $\log \sigma_{a,i}$ and $\log N_{f,i}$, respectively, while n is

the number of data items. For the classical linear regression, the value of B is approximated by its estimator, $\hat{B}$, in Equation 7:

$$\hat{B} = \frac{\sum_{i=1}^{n} \left(X_i - \bar{X}\right)\left(Y_i - \bar{Y}\right)}{\sum_{i=1}^{n} \left(X_i - \bar{X}\right)^2} \tag{7}$$

CLR aims to approximate the solution by minimising the sum of squares of the residuals between every data point and the regression line. The sum of squared vertical residuals for the CLR analysis, $\mathrm{E}_{\mathrm{CLR}}$, is calculated using Equation 8:

$$\mathrm{E}_{\mathrm{CLR}} = \sum_{i=1}^{n} \left(Y_i - \hat{Y}_i\right)^2 = \sum_{i=1}^{n} (Y_i - (A + BX_i))^2 \tag{8}$$

In the OLR, the estimator $\hat{B}$ is calculated using Equation 9, which involves variables W and Z.

$$\hat{B} = \frac{W + \sqrt{W^2 + Z^2}}{Z} \tag{9}$$

where,

- $Z = 2\sum_{i=1}^{n} \left(X_i - \bar{X}\right)\left(Y_i - \bar{Y}\right)$;
- $W = \sum_{i=1}^{n} \left(Y_i - \bar{Y}\right)^2 - \left(X_i - \bar{X}\right)^2$.

OLR calculates an optimal linear fit that minimises the sum of the squared Euclidean distances from the points to the regression line while accommodating uncertainties in both X and Y [67], in order to ensure robustness to outliers. The sum of the squared residuals for the OLR analysis, $\mathrm{E}_{\mathrm{OLR}}$, is defined by Equation 10.

$$\mathrm{E_{OLR}} = \sum_{i=1}^{n} d_i^2 = \sum_{i=1}^{n} \frac{\left(Y_i - \hat{Y}_i\right)^2}{B^2 + 1} \tag{10}$$

As mentioned, this study used local models to derive probabilistic fatigue curves for the different materials. The relationship between the regression parameters and the fatigue material parameters σ'_f and b is established through Equations 11 and 12:

$$\sigma'_f = 10^{-\frac{A}{B}} \tag{11}$$

$$b = 1/B \tag{12}$$

3.2. Methods for statistical analysis

3.2.1. ISO 12107 standard

ISO 12107 standard [68] outlines methodologies for planning fatigue tests and conducting statistical analyses of the resulting data. This standard has been adapted for determining the lower fatigue limit using statistical methods, assuming that the logarithm of fatigue life follows a normal distribution with a constant variance. The cumulative probability function (CDF) can be calculated using Equation 13:

$$p(x) = \frac{1}{\sigma_x \sqrt{2\pi}} \int_{-\infty}^{x} \exp\left[-\frac{1}{2}\left(\frac{x - \mu_x}{\sigma_x}\right)^2\right] dx \tag{13}$$

where, $x = \log N_f$, and μ_x and σ_x are the mean and standard deviation of x, respectively. Equation 14 defines the characteristic S-N curve, representing

the lower limit associated with probability of failure p_f for samples at a confidence level $(1-\alpha_n)$ and for a sample size n:

$$\log N_f = \hat{A} + \hat{B}\log\sigma_a - k_{(1-\alpha_n),p_f,n}\hat{s}\sqrt{1+\frac{1}{n}+\frac{(\log\sigma_a-\overline{\log\sigma_a})^2}{\sum_{i=1}^{n}\left(\log\sigma_{a,i}-\overline{\log\sigma_a}\right)^2}} \quad (14)$$

where, $\hat{B}$ and $\hat{A}$ denote the slope and intercept of the S-N curve, respectively, $k_{(1-\alpha_n),p_f,n}$ represents the one-sided tolerance limit for a normal distribution, which depends on the confidence level, $(1-\alpha_n)$, probability of failure, p_f, and sample size, n. The variables $\hat{s}$ and $\overline{\log\sigma_a}$ correspond to the standard deviation of the logarithm of fatigue life and the mean value of applied stress amplitude, respectively. The term within square root is a correction to the estimated standard deviation and depends on the number of tests and the range covered by the tests. When the number and range of tests are sufficiently large, the correction term approximates 1 and can be disregarded.

3.2.2. Two-parameter Weibull distribution

The two-parameter Weibull distribution, widely used for modelling reliability and lifetime data, including fatigue data [27, 28, 34, 35, 40] is recommended by international standards such as ISO 12107 [68] and ASTM E739 [69] standards, along with the normal distribution. The CDF of the two-parameter Weibull distribution is expressed by Equation 15:

$$F(x) = 1 - e^{\left(-\frac{x}{\alpha_{w_{(1-\alpha_n)}}}\right)^{\beta_{w_{(1-\alpha_n)}}}} \quad (15)$$

where $\alpha_{w_{(1-\alpha_n)}}$ is the Weibull scale parameter and $\beta_{w_{(1-\alpha_n)}}$ is the Weibull shape parameter, which depends on the confidence level, $(1-\alpha_n)$. The esti-

mation of confidence levels involves calculating the lower and upper bounds based on the assumed normal distribution of the estimated parameters.

For the determination of the scale and shape Weibull parameters, four different methods of estimation can be selected - Maximum Likelihood Method (MLM), Method of Moments (MM), Linear Least Square Method (LSM) and Weight Linear Least Squares Estimation Method (WLSM). Certain methods require a prior computation of the probability of failure, and in such cases, Benard's median rank estimator [70] is used, as defined by Equation 16:

$$\hat{F}\left(x\right) = \frac{i - 0.3}{n + 0.4} \tag{16}$$

where, i is the order number of failures and n denotes the sample size. Identifying an outperforming method is not straightforward, as it hinges on specific data characteristics, sample size and analysis objectives [27, 71]. For the sake of simplicity, the Maximum Likelihood Method was chosen in this study to derive the probabilistic fatigue curves, given its widespread use in modelling reliability data and fitting the Weibull distribution [35, 72–75]. The MLM involves estimating the maximum value of a defined likelihood function [75, 76]. For the Weibull distribution, the likelihood function, Equation 17, for a sample of independent and identically distributed observations $x_1, x_2, \ldots, x_n$ is expressed as:

$$\begin{aligned} L(\alpha_w, \beta_w \mid x) &= \prod_{i=1}^{n} f\left(x_i \mid \alpha_w, \beta_w\right) \\ &= \prod_{i=1}^{n} \left[\frac{\beta_w}{\alpha_w} \left(\frac{x_i}{\alpha_w} \right)^{(\beta_w - 1)} \exp\left\{ - \left(\frac{x_i}{\alpha_w} \right)^{\beta_w} \right\} \right] \end{aligned} \tag{17}$$

After that, this function is turned into a log-likelihood function by apply-

ing the natural ln, Equation 18, and the unknown parameters, α_w and β_w, are determined by maximising it.

$$\ln L(\alpha_w, \beta_w \mid x) = \sum_{i=1}^{n} \left[\ln \frac{\beta_w}{\alpha_w} + (\beta_w - 1) \ln \left(\frac{x}{\alpha_w} \right) - \left(\frac{x}{\alpha_w} \right)^{\beta_w} \right] \tag{18}$$

Upon estimation of the shape and scale parameters, the Equation 19 proposed by Júnior et al. [77] can be applied to derive probabilistic fatigue strength curves.

$$\log \sigma_a = \frac{\log \left(\frac{N_{\text{Norm}}}{\alpha_{w_{(1-\alpha_n)}} \left(-\ln\left(1-p_f\right) \right)^{1/\beta_{w(1-\alpha_n)}}} \right)}{B} - \frac{A}{B} \tag{19}$$

where, N_{Norm} is the normalised number of cycles, which is estimated using Equation 20:

$$N_{Norm} = \frac{N_f}{\bar{N}} \tag{20}$$

where, $\bar{N}$ is the average number of cycles to failure from the mean S-N curve, and N_f is the number of cycles to failure. Normalising the number of cycles is a common practice when computing fatigue curves based on the two-parameter Weibull distribution.

3.2.3. Castillo and Fernández-Canteli (CFC) model

Castillo and Fernández-Canteli (CFC) [34] introduced a three-parameter Weibull regression model suitable for variable stress ranges and fixed stress levels, such as stress R-ratio or mean stress. This model is ideal for high- or very-high cycle fatigue and is based on physical conditions and statistical requirements, with compatibility conditions between lifetime and stress

range distributions. Nevertheless, the model can be expressed taking into consideration the stress amplitude using Equation 21:

$$p_f(\log N_f; \log \sigma_a) = 1 - \exp\left\{ - \left[\frac{(\log N_f - B)(\log \sigma_a - C) - \lambda}{\delta} \right]^{\beta} \right\} \quad (21)$$
$$V = (\log N_f - B)(\log \sigma_a - C) \geq \lambda$$

where, p_f is the probability of failure, N_f represents the number of cycles to failure, σ_a is the stress amplitude, B is the threshold parameter for the lifetime ($B = \ln N_0$), C is threshold parameter for stress amplitude ($C = \ln \sigma_0$), also representing the conventional fatigue endurance limit, λ is the Weibull location parameter for normalised variable V, δ is the Weibull scale parameter, and β is the Weibull shape parameter. These parameters of can be estimated through several methods such as the maximum likelihood method, the probability-weighted moments [78] and the Castillo-Hadi method [79]. The *ProFatigue* software [80] was used to apply this model and obtain the probabilistic field for the experimental fatigue data. This software (developed by the authors of the model) simplifies the estimation of model parameters for any fatigue data.

3.2.4. Bayesian method based on Markov Chain Monte Carlo algorithm (MCMC)

Hierarchical Bayesian models have been applied to estimate the parameters of different probabilistic models for assessing fatigue life [81, 82]. The hierarchical Bayesian method requires numerical integration, typically using using methods like the Markov Chain Monte Carlo algorithm. The MCMC is a sampling method, that combines Monte Carlo simulation [83] and the

Markov chain [84], often used to estimate the posterior distribution of parameters in a probabilistic model. Among MCMC algorithms, Gibbs sampling is one of the most widely used for simulating Markov chains. It is a particular case of the Metropolis-Hastings algorithm [85, 86] and generates a multi-dimensional Markov chain by dividing the vector of random variables, θ, into subvectors, typically scalars, and sampling each subvector in turn, conditional on the most recent values of all other elements of θ [87]. This process involves iterative sampling from the conditional distributions of each variable within the distribution, given the current values of all other variables. To apply the Bayesian method with Gibbs sampling, the *OpenBugs* software was used [88, 89]. Equation 5 was reformulated, incorporating the random effect of materials and random errors in observations as a normal distribution:

$$Y = A + BX + \delta_i \tag{22}$$

where, $\delta_i = \sigma_i e_i$ with σ_i being the standard deviation of the logarithmic fatigue life under the stress level $\sigma_{a,i}$ and $e_i \sim$ Normal (0,1). According to the suggestion by Guida et al. [46], $u_i = \log \sigma_{a,i}$ and $\bar{u} = \frac{1}{n}\sum_{i=1}^{n} \log \sigma_{a,i}$, Equation 22 turns out as:

$$Y_i = A + BX_i + \text{Normal}\left(0, \sigma_i^2\right) \tag{23}$$

where, $Y_i = \log N_i, X_i = u_i - \bar{u}$. Equation 23 was modified to take into account a normal distribution with mean $\mu = A + BX_i$ and variance σ_i^2:

$$Y_{ij} \sim \text{Normal}\left(A + BX_i, \sigma_i^2\right) \tag{24}$$

or

$$Y_{ij} \sim \text{Normal}\left(\mu_i, \sigma_i^2\right) \text{ for } i = 1, \ldots, n \text{ and } j = 1, \ldots, m \tag{25}$$

where, $\mu_i = A + BX_i, Y_{ij}$ is the jth observation of the ith stress level. The prior distributions in the second stage assume $A|\mu_A, \sigma_A \sim \text{Normal}(\mu_A, \sigma_A^2)$, $B|\mu_B, \sigma_B \sim \text{Normal}(\mu_B, \sigma_B^2)$.

4. Results and discussion

This section presents a comparative analysis between different probabilistic S-N (p-S-N) curves derived using ISO 12107 standard [68], the two-parameter Weibull distribution, and a Bayesian method (MCMC), each incorporating either the classical linear regression (CLR) or the orthogonal linear regression (OLR) analysis. The Castillo-Fernández Canteli (CFC) model is also included for comparison with the proposed probabilistic models.

In the context of offshore structures and welded joints, where safety is of utmost importance, it is a common practice to assess fatigue curves while considering a probability of failure of 2.3% ($p_f = 2.3\%$) or 5% ($p_f = 5\%$) as benchmarks for evaluating fatigue life. These benchmarks align with the commonly used standards for steel structures, such as DNVGL-RP-C203 [57], the International Institute of Welding (IIW) [90], and Eurocode 3: Part 1-9 [56]. For the Eurocode 3: Part 1-9 [56] and for the International Institute of Welding [90] standards, the fatigue detail category, denoted as $\Delta\sigma_C$, assigns a numerical value to specific details for a given direction of stress fluctuation. This numerical designation indicates which design fatigue curve should be used to assess the fatigue strength of details. Typically, the category number aligns with the fatigue strength at a specified reference number of cycles,

which, in these cases, is $N_f = 2E6$ cycles. This estimation was conducted for a 75% confidence level with a 5% probability of failure, taking into account factors such as standard deviation, sample size, and residual stress effects. The DNVGL-RP-C203 standard [57] further recommends different types of S-N curves, derived from experimental fatigue tests, associated with a 2.3% probability of failure ($p_f = 2.3\%$), where the mean curve was determined with a 75% confidence level. The constant amplitude fatigue limit is assumed to be at $N_{f,0} = 5E6$ cycles for the Eurocode 3: Part 1-9 [56] and at $N_{f,0} = 1E7$ cycles for the DNVGL-RP-C203 [57] and IIW [90] standards.

4.1. Probabilistic fatigue strength curves for uncorroded materials

Figure 6 and 7 present the experimental fatigue results of the S355 base material and its p-S-N curves with a 5% probability of failure ($p_f = 5\%$), derived using the CLR and OLR analysis, respectively. In this section, it is important to recall that the probabilistic models adopted considered a confidence level of 75% in the parameters throughout the analysis.

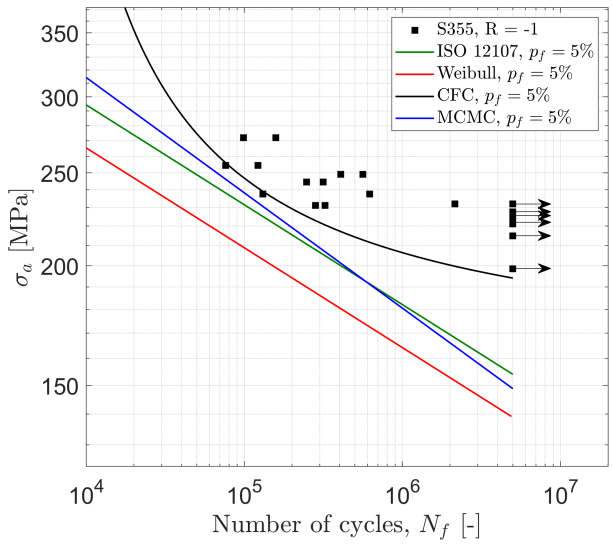

Figure 6: Comparison of all the p-S-N curves ($p_f = 5\%$) for the S355 base material using CLR.

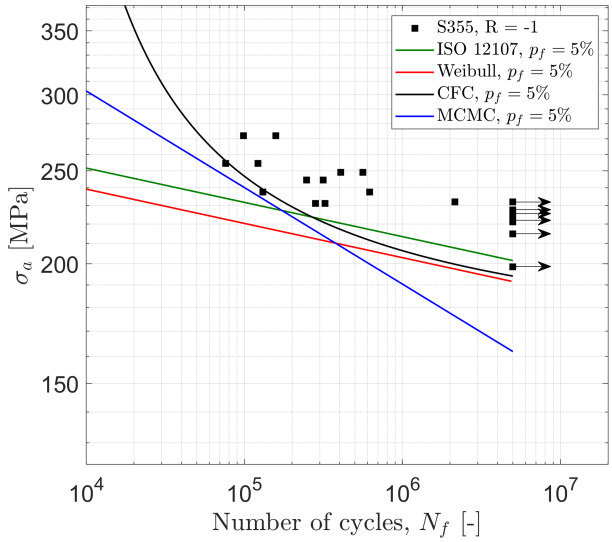

Figure 7: Comparison of all the p-S-N curves ($p_f = 5\%$) for the S355 base material using OLR.

Upon close examination of both figures, it is evident that the probabilistic fatigue curve derived through the Bayesian method (MCMC) almost aligns with the ISO 12107 standard [68] curve due to the application of the normal distribution in both models for CLR analysis. When it comes to OLR analysis combined with the Bayesian method (MCMC), this approach tends to underestimate fatigue life, particularly at high-stress levels. However, the Bayesian method (MCMC) using CLR analysis proves to be the least conservative model for the low-cycle fatigue regime. The fatigue curves obtained using the ISO 12107 standard [68] and a two-parameter Weibull distribution display similar characteristics for both regression analysis methods, with the CLR analysis curves being more conservative. Among the proposed models for the CLR, the fatigue curve obtained using the two-parameter Weibull distribution stands as the most conservative curve for all stress levels. Upon comparison between the curves obtained by both regression methods, the curves derived through CLR demonstrate a superior fit to the actual experimental data. This superiority is attributed to the lower sum of root mean square (RMSE) value associated with the CLR derived curves, presented in Table 4, underscoring their closer alignment with the observed fatigue data. The CFC model provides a non-linear p-S-N curve that effectively captures different trends in the experimental fatigue data, particularly in the transition between medium and high-cycle fatigue regimes. Nevertheless, it does not meet the safety design criteria, as at least one specimen from the experimental data falls outside the safety margins of the fatigue curve. Considering that offshore structures primarily face high-cycle fatigue loading, with a 5% probability of failure ($p_f = 5\%$) and to maintain safety margin levels

through regression analysis, the most suitable choice is the fatigue curve derived from the two-parameter Weibull distribution, specifically using CLR, and the Bayesian method (MCMC), specifically using OLR.

Similarly to the previous analysis, Figures 8 and 9 depict the experimental fatigue data of the S690QL base material (BM) and the corresponding p-S-N curves derived through the proposed probabilistic models for CLR and OLR analyses. The experimental fatigue data used in this probabilistic analysis was combined from both S690QL welded joints (J30 and J60).

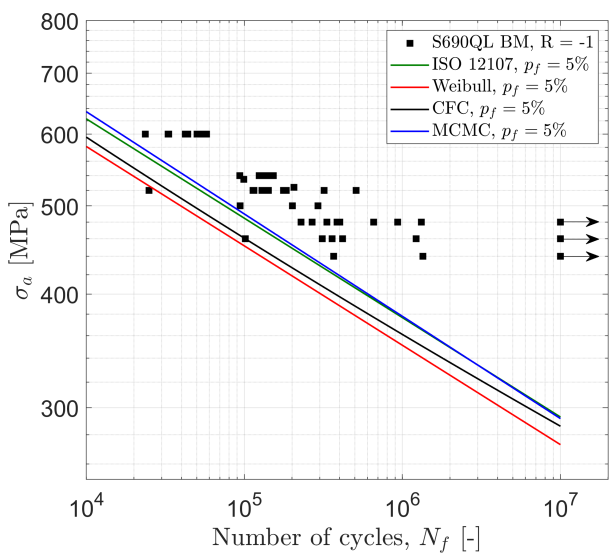

Figure 8: Comparison of all the p-S-N curves ($p_f = 5\%$) for the S690QL base material using CLR.

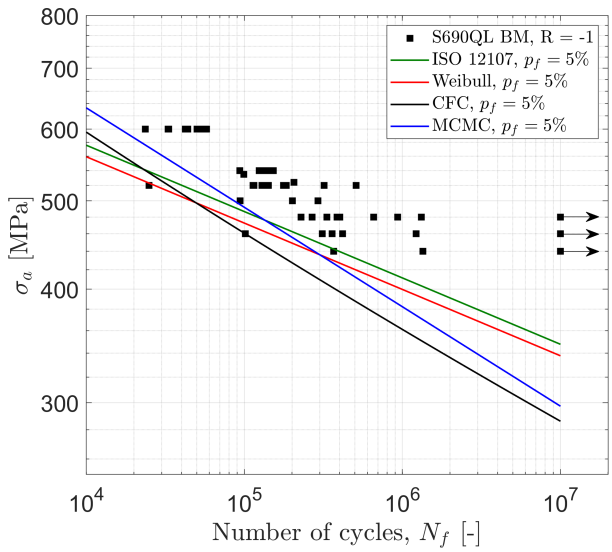

Figure 9: Comparison of all the p-S-N curves ($p_f = 5\%$) for the S690QL base material using OLR.

In Figure 8, it is also evident that the CLR analysis yields similar trend lines for the ISO 12107 standard [68] and the Bayesian method (MCMC) curves, primarily because both models use the normal distribution as the probabilistic distribution model. The Bayesian method (MCMC) curve offers a strong fit to the experimental data but appears less conservative, specifically in the medium-cycle fatigue regime, with some specimens falling outside the safety margins of the obtained probabilistic fatigue curve. Within CLR analysis, all proposed probabilistic curves maintain a similar trend line across various stress levels, with the two-parameter Weibull distribution curve as the most conservative among them. For the OLR analysis, the CFC model and the Bayesian method (MCMC) predict the most conservative results in the high-cycle fatigue regime. The CFC model proves to be the most con-

servative for the medium-cycle fatigue regime and its conservatism decreases as it approaches the low-cycle fatigue (LCF) regime.

Figures 10 and 11 showcase the experimental fatigue results of the S690QL welded steel material (WM) alongside the p-S-N curves derived using the proposed probabilistic models using the CLR and the OLR analyses, respectively. It is important to note that the fatigue data from both weld joints were combined to generate these curves, due to limited data availability.

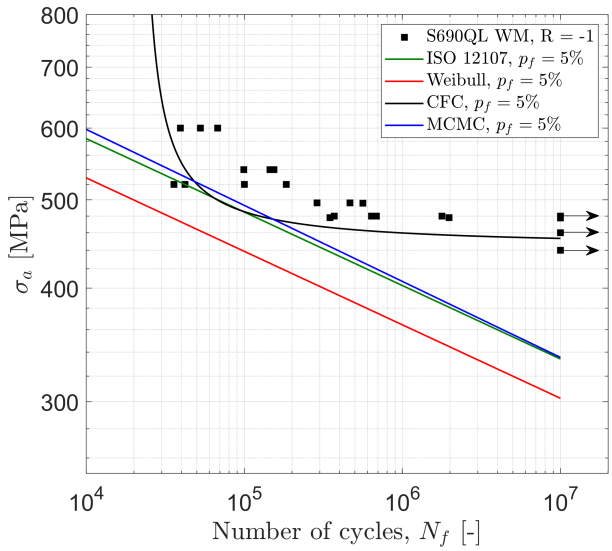

Figure 10: Comparison of all the p-S-N curves ($p_f = 5\%$) for the S690QL welded steel material using CLR.

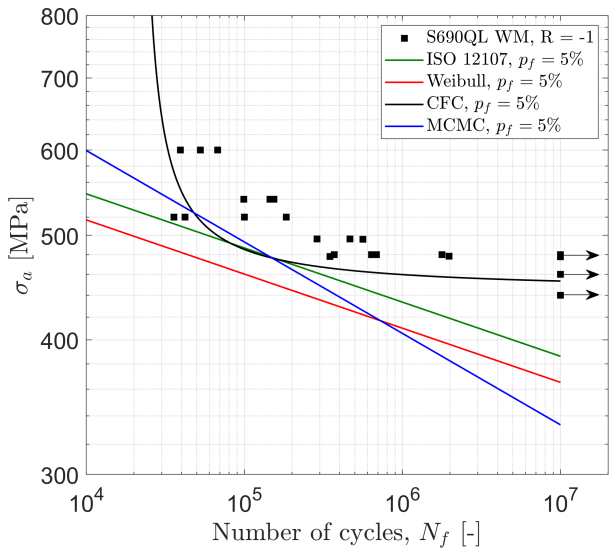

Figure 11: Comparison of all the p-S-N curves ($p_f = 5\%$) for the S690QL welded steel material using OLR.

In OLR analysis, the Bayesian method (MCMC) curve tends to overestimate fatigue life at low-stress levels, but it the most conservative and appropriate choice for the high-cycle fatigue regime. In contrast, at higher stress levels, the Bayesian method (MCMC) curve using OLR analysis tends to be less conservative when compared to the CLR analysis curve. To minimise fatigue data falling outside safety margins, the two-parameter Weibull distribution using CLR should be adopted as the most appropriate method to derive probabilistic fatigue curves for the weld material used in S690QL welded joints across all fatigue regimes. While the CFC model demonstrates a strong fit to the fatigue data at a 5% probability of failure ($p_f = 5\%$), caution is advised given that some specimen results closely align with the curve. Additionally, the CFC model seems to accurately predict the constant ampli-

tude fatigue limit, aligning with the observed run-out fatigue data presented in Appendix A.

Table 3 presents the parameters used to define the CFC model for both the S355 and S690QL base and welded steels.

Table 3: Parameters defining the CFC model for each material.

Material	**B**	**C**	N_0	σ_0	λ	δ	β
S355	7.78	5.04	2395	154.38	1.64	0.62	1.77
S690QL - BM	-82.95	-4.11	≈ 0	≈ 0	964.70	15.00	1.91
S690QL - WM	9.92	6.09	20333	441.42	-0.68	1.01	15.00

Table 4 summarises the material parameters for the fatigue strength curves of both S355 and S690QL base and welded steels, according to each probabilistic and regression model corresponding to probabilities of failure of $p_f = 2.3\%, p_f = 5\%$, and $p_f = 50\%$ (mean curve). The sum of the root mean square error (RMSE) in the X-axis ($\log N_f$) is also provided as a measure of the model's accuracy.

Table 4: Summary of the material parameters for the S355 and for the S690QL base and welded steels, according to each probabilistic and regression model.

Material	**Probabilistic model**	**Regression model**	**RMSE** ($\log N_f$)	σ'_f **[MPa]**				$\boldsymbol{b}$	$CV_{\sigma'_f}$
				p_f **= 2.3%**	p_f **= 5%**	p_f **= 50%**	**StD**		
S355	ISO 12107	CLR	0.306	742.57	767.88	906.99	31.44	-0.104	0.035
		OLR	0.522	342.94	349.73	385.53	7.82	-0.036	0.020
	Weibull distribution	CLR	0.306	642.40	692.48	906.99	91.63	-0.104	0.101
		OLR	0.522	319.01	332.50	385.53	33.00	-0.036	0.086
	Bayesian method (MCMC)	$\text{CLR}_{\text{Bayesian}}$	-	921.00	951.44	1108.27	44.63	-0.120	0.040
		$\text{OLR}_{\text{Bayesian}}$	-	745.58	765.83	868.45	28.83	-0.101	0.033
S690QL - BM	ISO 12107	CLR	0.255	1664.71	1706.43	1924.53	54.90	-0.109	0.029
		OLR	0.312	1105.13	1127.70	1243.99	28.95	-0.073	0.023
	Weibull distribution	CLR	0.255	1504.35	1590.97	1924.53	149.45	-0.109	0.078
		OLR	0.312	1054.14	1095.29	1243.99	69.48	-0.073	0.056
	Bayesian method (MCMC)	$\text{CLR}_{\text{Bayesian}}$	-	1747.96	1789.86	2000.18	58.68	-0.113	0.029
		$\text{OLR}_{\text{Bayesian}}$	-	1694.51	1733.41	1928.41	54.27	-0.109	0.028
S690QL - WM	ISO 12107	CLR	0.322	1198.38	1229.23	1393.37	38.36	-0.081	0.028
		OLR	0.409	850.57	867.77	957.82	20.77	-0.050	0.022
	Weibull distribution	CLR	0.322	1112.79	1170.02	1393.37	96.99	-0.081	0.070
		OLR	0.409	785.38	820.74	957.82	69.34	-0.050	0.072
	Bayesian method (MCMC)	$\text{CLR}_{\text{Bayesian}}$	-	1261.62	1291.10	1438.89	41.17	-0.084	0.029
		$\text{OLR}_{\text{Bayesian}}$	-	1278.87	1309.07	1460.65	42.25	-0.085	0.029

The higher coefficient of variation (CV) between the two-parameter Weibull distribution and the other models can be attributed to the shape of their respective probability density functions. The Weibull distribution has a heavier tail compared to the normal distribution, resulting in a wider spread of data points and thus a higher standard deviation. This discrepancy can be explained by the fact that the two-parameter Weibull distribution allows for a non-linear relationship between the stress amplitude σ_a and the number of cycles N_f, whereas the normal distribution assumes a linear relationship. Also, a higher CV results in larger safety margins, accommodating a wider spectrum of loading conditions.

4.2. Probabilistic fatigue strength curves for corroded materials

To account for the influence of corrosion on the probabilistic modelling of fatigue strength data, Equation 2 must be applied. Due to limited experimental fatigue results for materials affected by corrosion, it is necessary to reference relevant literature. Several authors [52, 91, 92] have conducted fatigue testing on multiple grades of both uncorroded and corroded steels. By considering the constant amplitude fatigue limit for each uncorroded material, as indicated in Table 6 for $N_{f,0}$ = 1E7 cycles, and establishing the ratio of $\sigma_{0,\text{cor}}/\sigma_0 = 0.37$ for the S355 mild steel, and $\sigma_{0,\text{cor}}/\sigma_0 = 0.27$ for the S690QL base and weld steels from [53, 93], the corroded constant amplitude fatigue limit, $\sigma_{0,\text{cor}}$, was calculated for each material.

To estimate the number of cycles, $N_{f,y}$, at the yield strength, σ_y, the most conservative uncorroded probabilistic models from Section 4.1 were taken into account. These models were evaluated from the high-cycle fatigue region for each material. Table 5 presents the corresponding number of cycles, $N_{f,y}$, at the yield strength, σ_y, for both S355 and S690QL base and welded steels.

Table 5: Number of cycles ($N_{f,y}$) at the yield strength (σ_y) for both S355 and S690QL base and welded steels.

Material	**Regression model**	**Probabilistic model**	$p_f = 2.3\%$	$p_f = 5\%$	$p_f = 50\%$
S355	CLR	Weibull distribution	216	444	4769
	OLR	Bayesian method (MCMC)	1136	1483	5166
S690QL - BM	CLR	Weibull distribution	379	632	3414
	OLR	Bayesian method (MCMC)	1121	1380	3655
S690QL - WM	CLR	Weibull distribution	122	226	1746
	OLR	Bayesian method (MCMC)	499	658	2393

Table 6 provides the uncorroded constant amplitude fatigue limits, σ_0, for both S355 and S690QL base and welded steels. The results are based on

each probabilistic and regression model, and are given for different defined numbers of cycles.

Table 6: Constant amplitude fatigue limit (σ_0) for the S355 and S690QL base and weld steels, according to each probabilistic and regression model.

Material	**Regression model**	**Probabilistic model**	**Constant amplitude fatigue limit, σ_0 [MPa]**					
			$N_{f,0}$ = 5E6 cycles			$N_{f,0}$ = 1E7 cycles		
			$p_f = 2.3\%$	$p_f = 5\%$	$p_f = 50\%$	$p_f = 2.3\%$	$p_f = 5\%$	$p_f = 50\%$
S355	CLR	Weibull distribution	128.83	138.88	177.85	119.86	129.21	165.46
	OLR	Bayesian method (MCMC)	157.62	161.90	183.59	146.99	150.98	171.21
S690QL - BM	CLR	Weibull distribution	278.55	294.59	354.24	258.22	273.09	328.39
	OLR	Bayesian method (MCMC)	313.47	320.67	356.74	290.58	297.25	330.69
S690QL - WM	CLR	Weibull distribution	319.92	336.38	396.80	302.49	318.05	375.18
	OLR	Bayesian method (MCMC)	345.65	353.81	394.78	325.91	333.61	372.24

The probabilistic corroded fatigue curves were established based on Equation 2. The estimated corroded data points were determined from the newly established corroded curve. However, to precisely generate postulated corroded data points from these first estimated corroded data points, the root mean square error (RMSE) of the deviations between the experimental data and the predicted values, according to the used uncorroded probabilistic model, was considered. These postulated data points are identified with an asterisk (*) in the legend of each figure.

Figure 12 and Figure 13 depict the corroded and uncorroded probabilistic fatigue curves for the S355 base material using CLR and OLR for a 50% probability of failure ($p_f = 50\%$), respectively. The uncorroded constant amplitude fatigue limits, σ_0, for the S355 base material are 165.46 MPa (CLR) and 171.20 MPa (OLR). Correspondingly, the corroded constant amplitude fatigue limits, $\sigma_{0,\mathrm{cor}}$, are 62.62 MPa (CLR) and 63.35 MPa (OLR).

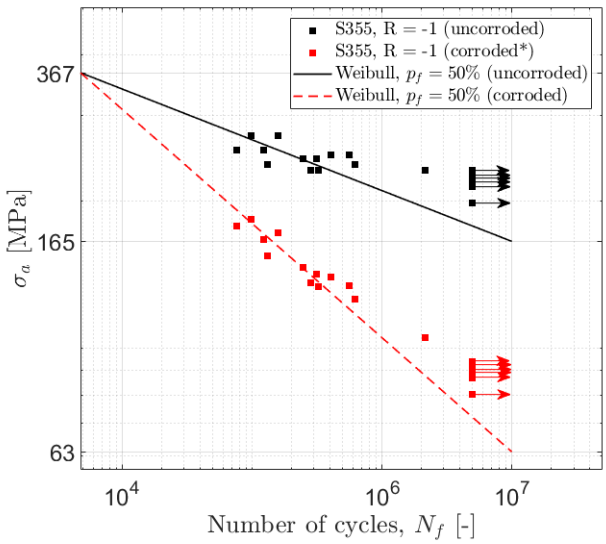

Figure 12: Uncorroded and corroded p-S-N curves ($p_f = 50\%$) with experimental uncorroded and postulated corroded* data for the S355 base material using CLR.

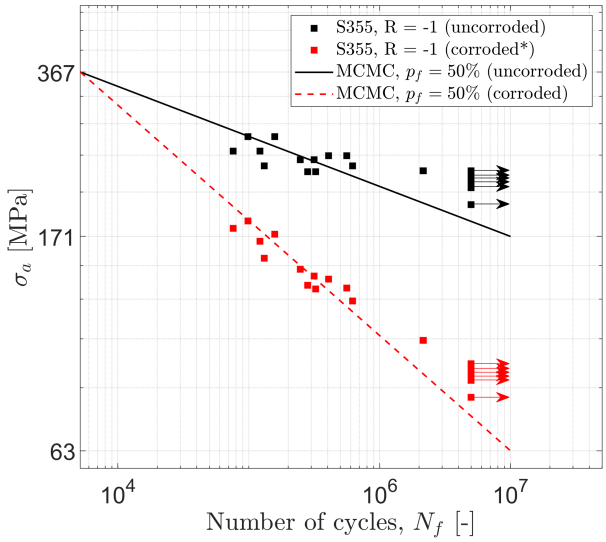

Figure 13: Uncorroded and corroded p-S-N curves ($p_f = 50\%$) with experimental uncorroded and postulated corroded* data for the S355 base material using OLR.

Figure 14 and Figure 15 show the corroded and uncorroded probabilistic mean fatigue strength curves for the S690QL base material using CLR and OLR, respectively. For CLR analysis, the uncorroded constant amplitude fatigue limit for the S690QL base material is 328.38 MPa. The corroded constant amplitude fatigue limit for the same material, under CLR analysis, is 89.41 MPa. Similarly, for OLR analysis, the uncorroded constant amplitude fatigue limit is 330.69 MPa, and the corroded constant amplitude fatigue limit is 89.50 MPa.

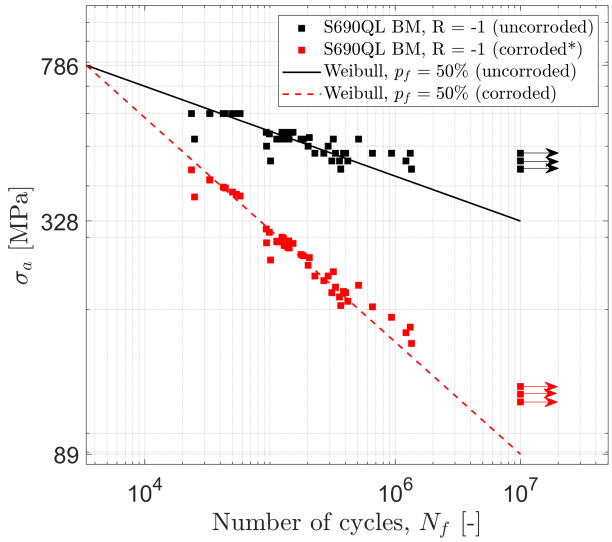

Figure 14: Uncorroded and corroded p-S-N curves ($p_f = 50\%$) with experimental uncorroded and postulated corroded* data for the S690QL base material using CLR.

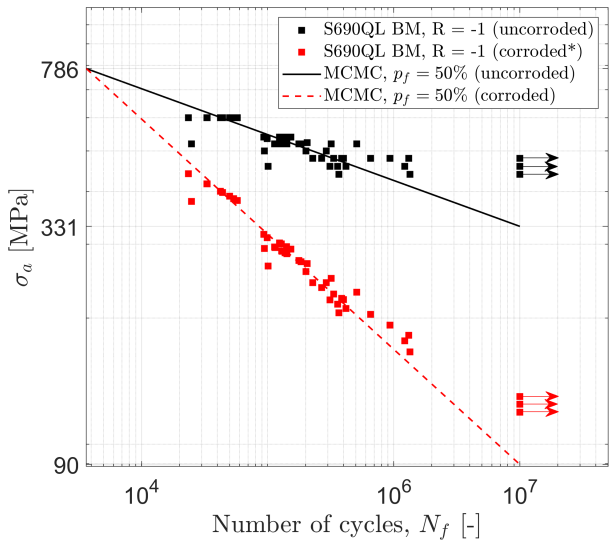

Figure 15: Uncorroded and corroded p-S-N curves ($p_f = 50\%$) with experimental uncorroded and postulated corroded* data for the S690QL base material using OLR.

Figure 16 and Figure 17 present the mean probabilistic fatigue strength curves for the S690QL welded steel, both for corroded and uncorroded conditions, using CLR and OLR, respectively. Based on CLR analysis, the constant amplitude fatigue limits for uncorroded and corroded S690QL welded steel are 375.18 MPa and 101.54 MPa, respectively. Similarly, through OLR analysis, the uncorroded constant amplitude fatigue limit remains at 372.24 MPa, whereas the corroded constant amplitude fatigue limit is 100.75 MPa.

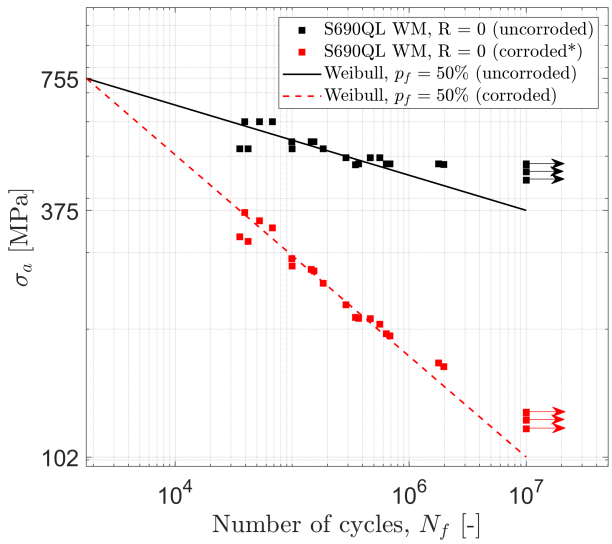

Figure 16: Uncorroded and corroded p-S-N curves ($p_f = 50\%$) with experimental uncorroded and postulated corroded* data for the S690QL welded steel using CLR.

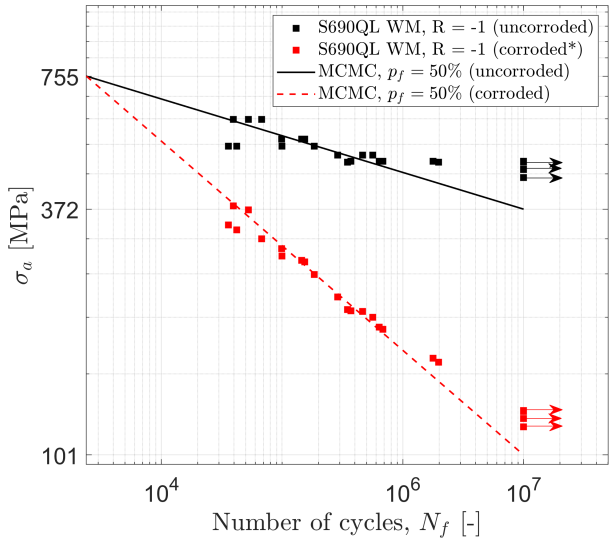

Figure 17: Uncorroded and corroded p-S-N curves ($p_f = 50\%$) with experimental uncorroded and postulated corroded* data for the S690QL welded steel using OLR.

4.3. Proposed fatigue strength curves

For the derivation of probabilistic fatigue curves, it is important to propose curves that cover the entire range of a typical fatigue response (across distinct scenarios). Standards such as Eurocode 3: Part 1-9 [56], DNVGL-RP-C203 [57] and IIW [90] define different limits for constant or variable amplitude fatigue limits, ensuring safety against fatigue failure. Typically, this is at $N_{f,0}$ = 5E6 cycles, according to Eurocode 3: Part 1-9 [56], and $N_{f,0}$ = 1E7 cycles, according to DNVGL-RP-C203 [57]. The variable amplitude fatigue limit, also known as the cut-off fatigue limit, refers to the specific number of cycles below which the material or detail is considered to have an infinite fatigue life under variable amplitude loading. Eurocode 3: Part 1-9 [56] and DNVGL-RP-C203 [57] set the cut-off limit at $N_{f,0,L}$ = 1E8 cycles. In contrast, IIW [90] guidelines designates the variable amplitude fatigue limit similarly to the constant amplitude fatigue limit at $N_{f,0,L}$ = 1E7 cycles.

Equation 26, based on the Eurocode 3: Part 1-9 [56] and DNVGL-RP-C203 [57], proposes a relationship to relate the uncorroded constant amplitude fatigue limit, σ_0, to the uncorroded variable fatigue limit, $\sigma_{0,L}$.

$$\sigma_{0,L} = \left(\frac{N_{f,0}}{N_{f,0,L}}\right)^{b_L} \sigma_0 \tag{26}$$

where, $N_{f,0}$ represents the number of cycles for a constant amplitude fatigue limit, σ_0, according to each standard, and $N_{f,0,L}$ represents the number of cycles for the variable fatigue limit, $\sigma_{0,L}$, based on each standard. The parameter b_0 denotes the inverse slope of the constant amplitude fatigue limit, defined as $1/m$, where m is 3, in both Eurocode 3: Part 1-9 [56] and DNVGL-RP-C203 [57] standards. The inverse slope of the variable amplitude fatigue

limit for the material, b_L, can be estimated using Equation 27.

$$b_L = -\frac{b}{2b_0 + 1} \tag{27}$$

Equation 28 adapts the proposed relationship to the corroded curve, estimating the corroded variable amplitude fatigue limit, $\sigma_{0,L_{\text{cor}}}$, using the same approach.

$$\sigma_{0,L_{\text{cor}}} = \left(\frac{N_{f,0}}{N_{f,0,L}}\right)^{b_{L,\text{cor}}} \sigma_{0,\text{cor}} \tag{28}$$

Considering b_{cor} equal to $(b - c)$, as presented in Equation 2, $b_{L,\text{cor}}$ can be expressed using Equation 29.

$$b_{L,\text{cor}} = -\frac{b_{\text{cor}}}{2b_0 + 1} \tag{29}$$

Taking into account the most conservative probabilistic model from the CLR analysis and the proposed relationships, Figures 18 to 20 present the proposed fatigue strength curves for the S355 and S690QL base and welded steels, respectively, for different probabilities of failure. The parameters required to establish the fatigue strength curves for the S355 and S690QL base and welded steels, based on the most conservative probabilistic model from the OLR analysis, can be found in Table 7.

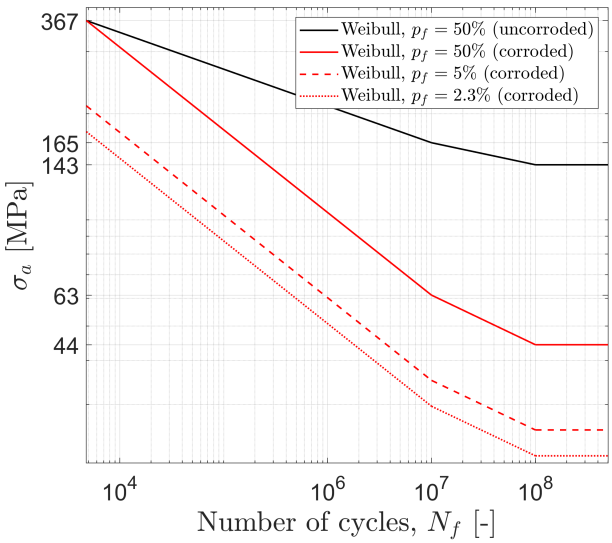

Figure 18: Proposed uncorroded and corroded fatigue strength curves for the S355 base material using CLR.

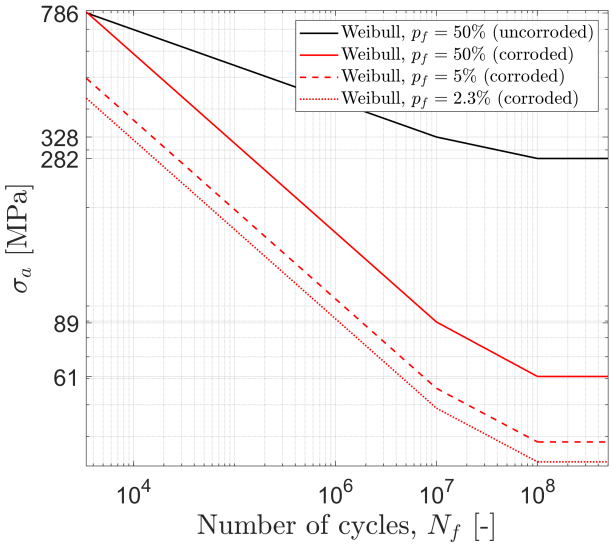

Figure 19: Proposed uncorroded and corroded fatigue strength curves for the S690QL base material using CLR.

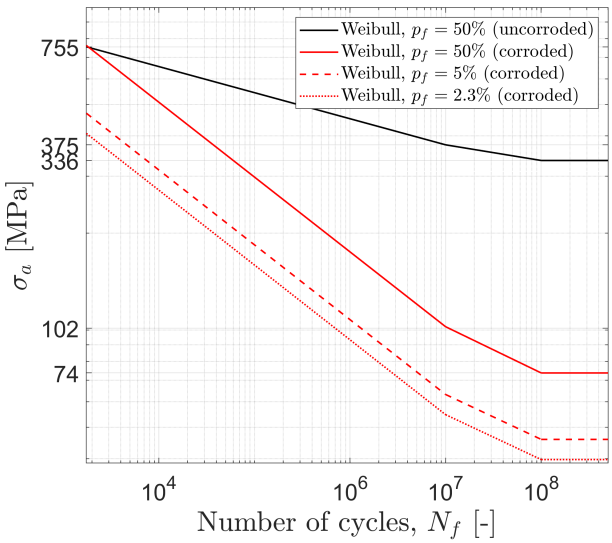

Figure 20: Proposed uncorroded and corroded fatigue strength curves for the S690QL welded steel using CLR.

Table 7 provides a summary of the estimated parameters for deriving the proposed corroded fatigue strength curves, taking into account the most conservative probabilistic model for CLR and OLR. It is important to highlight that $\sigma'_{f,\text{cor}} = \sigma'_f N^c_{f,y}$ and $b_{\text{cor}} = b - c$ considering Equation 2.

Table 7: Overview of the parameters used for the proposed corroded fatigue strength curves, considering CLR and OLR for each material.

				CLR	**OLR**
S355	$\sigma'_{f,\text{cor}}$ [MPa]	$p_f = 2.3\%$		1291.96	1878.89
		$p_f = 5\%$		1529.50	1998.53
		$p_f = 50\%$		2727.64	2670.19
	b_{cor}			-0.234	-0.232
	$\sigma_{0,\text{cor}}$ [MPa]	$p_f = 50\%$	$N_{f,0}$ = 5E6 cycles	73.65	74.41
			$N_{f,0}$ = 1E7 cycles	62.62	63.35
	$\sigma_{0,L}$ [MPa]	$p_f = 50\%$	$N_{f,0}$ = 5E6 cycles	147.48	153.18
			$N_{f,0}$ = 1E7 cycles	143.28	148.96
	$\sigma_{0,L_{\text{cor}}}$ [MPa]	$p_f = 50\%$	$N_{f,0}$ = 5E6 cycles	48.35	49.02
			$N_{f,0}$ = 1E7 cycles	45.31	45.97
S690QL - BM	$\sigma'_{f,\text{cor}}$ [MPa]	$p_f = 2.3\%$		3976.67	5403.21
		$p_f = 5\%$		4573.39	5719.89
		$p_f = 50\%$		7291.57	7474.30
	b_{cor}			-0.273	-0.275
	$\sigma_{0,\text{cor}}$ [MPa]	$p_f = 50\%$	$N_{f,0}$ = 5E6 cycles	108.04	108.26
			$N_{f,0}$ = 1E7 cycles	89.41	89.50
	$\sigma_{0,L}$ [MPa]	$p_f = 50\%$	$N_{f,0}$ = 5E6 cycles	291.04	293.06
			$N_{f,0}$ = 1E7 cycles	282.35	284.30
	$\sigma_{0,L_{\text{cor}}}$ [MPa]	$p_f = 50\%$	$N_{f,0}$ = 5E6 cycles	66.13	66.10
			$N_{f,0}$ = 1E7 cycles	61.31	61.25
S690QL - WM	$\sigma'_{f,\text{cor}}$ [MPa]	$p_f = 2.3\%$		2297.48	3386.98
		$p_f = 5\%$		2653.02	3619.76
		$p_f = 50\%$		4302.28	4945.37
	b_{cor}			-0.232	-0.241
	$\sigma_{0,\text{cor}}$ [MPa]	$p_f = 50\%$	$N_{f,0}$ = 5E6 cycles	120.39	119.11
			$N_{f,0}$ = 1E7 cycles	101.54	100.75
	$\sigma_{0,L}$ [MPa]	$p_f = 50\%$	$N_{f,0}$ = 5E6 cycles	343.15	338.96
			$N_{f,0}$ = 1E7 cycles	335.55	331.08
	$\sigma_{0,L_{\text{cor}}}$ [MPa]	$p_f = 50\%$	$N_{f,0}$ = 5E6 cycles	79.36	77.16
			$N_{f,0}$ = 1E7 cycles	74.42	72.16

5. Concluding remarks

This work applies different probabilistic models to compare and derive fatigue strength curves for S355 and for S690QL base and welded steels. The probabilistic fatigue models, including the ISO 12107 standard [68], the two-parameter Weibull distribution and the Bayesian method (MCMC), were utilised under two different linear regression analysis methods. Additionally, the non-linear Castillo and Fernandéz-Canteli (CFC) model was applied for comparison. The material's applicability was highlighted as a major factor in selecting the appropriate probabilistic curve, especially in contexts like offshore structures subjected to high-frequency cyclic loads with relatively low-stress levels. Corroded probabilistic curves were proposed based on the selected probabilistic models. When it comes to choosing between classical and orthogonal linear regression for fatigue design, there are a few factors to consider. For new project design, classical linear regression may be the more appropriate choice as it can provide a clear understanding of the relationship between different design factors and the fatigue life of a system. However, for retrofitting purposes, where there may be uncertainty or error in the data, orthogonal linear regression may be a more suitable option as it takes these factors into account. The primary objective of this study was to analyse fatigue experimental data from diverse sources of fatigue tests involving steels, commonly used in the offshore industry, in order to establish reliable uncorroded and corroded proposals of fatigue strength curves to characterise these materials. Related to this study, the following key findings and conclusions can be stated:

- The orthogonal linear regression (OLR) analysis showed a more con-

servative fit compared to classical linear regression (CLR) analysis at high-stress levels (LCF regime).

- In both regression analyses, the coefficient of variation (CV) estimated from the curves based on the ISO 12107 standard [68] was below 0.05. As a result, the recommended CV value in existing literature is conservative and appropriate, ensuring larger safety margins.

- Among the proposed linear probabilistic models, the Bayesian method (MCMC) using a CLR analysis yielded the least conservative curve for all fatigue regimes. Conversely, the two-parameter Weibull curve with a CLR analysis presented the most conservative fit for medium- and high-cycle fatigue regimes;

- In the other hand, the Bayesian method (MCMC) using a OLR analysis presents the most conservative curve for the high-cycle fatigue regime.

- The probabilistic curve from the ISO 12107 standard [68] displayed an approximate trend line compared to the Bayesian method (MCMC) using CLR analysis, due to the normal distribution being the distribution model, especially for the S690QL base material where they are practically aligned and overlapped;

- While the CFC model provides advantages, such as allowing the accurate prediction of the constant amplitude fatigue limit, it yields some non-conservative results. Nevertheless, it demonstrates a strong fit and potential for the high-cycle fatigue regime, as long as there are no asymptotes that limit curve fitting.

- Corroded fatigue strength curves were proposed for the S355 and S690QL base and welded steels based on the most conservative probabilistic models in the high-cycle fatigue regime (N_f = 1E7 cycles).

- A decrease in the ratio between the corroded and uncorroded constant amplitude fatigue limit corresponds to an increase in the difference between the corroded and uncorroded variable amplitude fatigue limit, accompanied by a more pronounced steepness in the proposed corroded fatigue curve.

- It is noteworthy that the corroded fatigue strength coefficient is markedly high, which ensures that both the corroded and uncorroded condition curves exhibit the same number of cycles at the yield strength. The corroded curve displays a steeper slope, indicative of accelerated degradation,, meaning that the material's fatigue life and resistance to cyclic loading deteriorate more rapidly under corrosive conditions. This effect highlights the increased susceptibility of the material to fatigue failure due to the combined effects of mechanical loading and the corrosive environment.

- When considering the fatigue design for new systems using CLR, the two-parameter Weibull distribution is recommended. However, if the objective is to extend the lifespan the OLR should be used and the Bayesian approach (MCMC) is suggested as the most feasible option, taking advantage of the fatigue resistant capacity of long term operated materials and structures without jeopardising the retrofitting project.

Declaration of competing interest

The authors declare that they have no known competing financial interests or personal relationships that could have appeared to influence the work reported in this manuscript.

Credit authorship contribution statement

Paulo Mendes: Conceptualization, Formal analysis, Investigation, Methodology, Validation, Writing – original draft and Writing – review & editing. **José A.F.O Correia**: Formal analysis, Investigation, Resources, Supervision, Validation, Writing – original draft and Writing – review & editing **António Mourão**: Formal analysis, Validation, Writing – original draft and Writing – review & editing. **Rita Dantas**: Investigation, Validation, Writing – original draft and Writing – review & editing **Abílio de Jesus**: Resources, Supervision, Validation and Writing – review & editing. **Claúdio Horas**: Validation, Visualization and Writing – review & editing. **Nicholas Fantuzzi**: Supervision, Validation and Writing – review & editing. **Lance Manuel**: Supervision, Validation and Writing – review & editing.

Acknowledgements

This research was supported by the project grant AARM 4.0 - Aços de Alta Resistência na Metalomecânica 4.0 with the reference POCI-01-0247-FEDER-068492, co-financed by the European Regional Development Fund (ERDF), through the Operational Programme for Competitiveness and Internationalization (COMPETE2020), under the PORTUGAL 2020 Partnership Agreement. This work was financially supported by: Base Funding -

UIDB/04708/2020 with DOI 10.54499/UIDB/04708/2020 (https://doi.org/10.54499/UIDB/04708/2020) and Programmatic Funding - UIDP/04708/2020 with DOI 10.54499/UIDP/04708/2020 (https://doi.org/10.54499/UIDP/04708/2020) of the CONSTRUCT - Instituto de I&D em Estruturas e Construções - funded by national funds through the FCT/MCTES (PIDDAC). The author José A.F.O. Correia gratefully acknowledges the financial support by MIT-EXPL/SOE/0054/2021 - Hyperloop-Verne - Exploratory Analysis of Biomimetic-inspired Oceanic Hyperloop Transport Infrastructures. José A.F.O. Correia would like to thank the individual project grant (2020.03856.CEECIND) awarded by national funds (PIDDAC) through the Portuguese Science Foundation (FCT/MCTES). This work is also a result of Agenda "NEXUS: Innovation Pact Digital and Green Transition – Transports, Logistics and Mobility", nr. C645112083-00000059, investment project nr. 53, financed by the Recovery and Resilience Plan (PRR) and by European Union - NextGeneration EU. Finally, this research work (reference SFRH/BD/151377/2021) is also co-financed by the Social European Fund – through the Northern Regional Operational Program (NORTE 2020), the Regional Operational Program of the Center (Centro 2020) and the Regional Operational Program of Alentejo (Alentejo 2020) - and by the Portuguese Foundation for Science and Technology – FCT under MIT Portugal.

Appendix A. Experimental fatigue data

Table A.8: Pure axial fatigue data for the S355 mild steel.

Specimen	Number of cycles, N_f	Stress ratio, R	Stress amplitude, σ_a [MPa]	Normalised stress amplitude, $\sigma_{a_{norm}}$ [MPa]	Runout
1	5.00E+06	0.01	168.30	198.40	1 (excluded)
6	5.00E+06	0.01	182.16	214.74	1 (excluded)
7	5.00E+06	0.01	187.61	221.16	1 (excluded)
8	5.00E+06	0.01	190.58	224.66	1 (excluded)
9	5.00E+06	0.01	193.05	227.58	1 (excluded)
4	3.24E+05	0.01	196.02	231.08	
5	2.82E+05	0.01	196.02	231.08	
11	6.21E+05	0.01	201.47	237.50	
12	1.31E+05	0.01	201.47	237.50	
21	2.47E+05	0.01	207.41	244.50	
22	3.16E+05	0.01	207.41	244.50	
19	1.22E+05	0.01	215.82	254.42	
20	7.61E+04	0.01	215.82	254.42	
18	5.00E+06	-1	232	232	1 (excluded)
17	2.15E+06	-1	232	232	
14	5.62E+05	-1	249	249	
16	4.07E+05	-1	249	249	
13	1.58E+05	-1	272	272	
15	9.86E+04	-1	272	272	

Table A.9: Rotating bending fatigue results for the S690QL base material, R = -1 (Specimen 1 to Specimen 33).

Specimen	Number of cycles, N_f	Stress amplitude, σ_a [MPa]	Runout
1	1.15E+05	520	
2	1.84E+05	520	
3	1.42E+05	520	
4	2.92E+05	500	
5	1.14E+05	520	
6	9.41E+04	500	
7	1.00E+07	440	1 (excluded)
8	4.18E+05	460	
9	1.00E+07	440	1 (excluded)
10	1.35E+06	440	
11	3.12E+05	460	
12	3.68E+05	440	
13	4.24E+04	600	
14	1.31E+05	520	
15	5.00E+04	600	
16	9.35E+04	540	
17	5.39E+04	600	
18	1.53E+05	540	
19	1.28E+05	540	
20	4.01E+05	480	
21	3.59E+05	460	
22	2.28E+05	480	
23	2.68E+05	480	
24	2.02E+05	500	
25	9.90E+04	535	
26	2.06E+05	524	
27	1.41E+05	540	
28	1.38E+05	520	
29	5.09E+05	520	
30	3.20E+05	520	
31	5.76E+04	600	
32	3.32E+04	600	
33	5.75E+04	600	

Table A.10: Rotating bending fatigue results for the S690QL base material, R = -1 (Specimen 34 to Specimen 56).

Specimen	Number of cycles, N_f	Stress amplitude, σ_a [MPa]	Runout
34	6.57E+05	480	
35	1.31E+06	480	
36	3.33E+05	480	
37	1.00E+07	440	1 (excluded)
38	1.00E+07	440	1 (excluded)
39	1.00E+07	440	1 (excluded)
40	1.24E+05	540	
41	1.13E+05	520	
42	2.49E+04	520	
43	1.29E+05	520	
44	1.77E+05	520	
45	3.86E+05	480	
46	1.00E+07	480	1 (excluded)
47	9.33E+05	480	
48	4.39E+04	600	
49	2.36E+04	600	
50	3.30E+04	600	
51	1.00E+07	460	1 (excluded)
52	1.22E+06	460	
53	1.01E+05	460	
54	1.00E+07	440	1 (excluded)
55	1.00E+07	440	1 (excluded)
56	1.00E+07	440	1 (excluded)

Table A.11: Rotating bending fatigue results for the S690QL welded steel, R = -1.

Specimen	Number of cycles, N_f	Stress amplitude, σ_a [MPa]	Runout
1	1.00E+07	480	1 (excluded)
2	1.00E+07	480	1 (excluded)
3	1.00E+07	480	1 (excluded)
4	1.78E+05	480	
5	1.84E+05	520	
6	9.98E+04	520	
7	3.58E+04	520	
8	4.21E+04	520	
9	3.70E+05	480	
10	3.94E+04	600	
11	6.38E+05	480	
12	5.27E+04	600	
13	6.85E+05	480	
14	6.78E+04	600	
15	1.00E+07	477.57	1 (excluded)
16	3.48E+05	478.01	
17	1.98E+06	478.17	
18	5.63E+05	496.02	
19	2.88E+05	496.08	
20	4.65E+05	496.12	
21	1.54E+05	540	
22	1.45E+05	540	
23	9.91E+04	540	
24	1.00E+07	440	1 (excluded)
25	1.00E+07	440	1 (excluded)
26	1.00E+07	460	1 (excluded)

References

[1] S. Pennock, A. Garcia-Teruel, D. R. Noble, O. Roberts, A. de Andres, C. Cochrane, H. Jeffrey, Deriving current cost requirements from future targets: Case studies for emerging offshore renewable energy technologies, Energies 15 (2022).

[2] G. Colaleo, F. Nardo, A. Azzellino, D. Vicinanza, Decommissioning of offshore platforms in adriatic sea: The total removal option from a life cycle assessment perspective, Energies 15 (2022).

[3] I. Legorburu, K. R. Johnson, S. A. Kerr, Multi-use maritime platforms-north sea oil and offshore wind: Opportunity and risk, Ocean & Coastal Management 160 (2018) 75–85.

[4] S. R. Kolian, J. M. M. Torres, R. M. Garcia, J. M. D. Guzman, Alternate uses of retired oil and gas platforms in the gulf of mexico, Renewable Energy 139 (2020) 1147–1155.

[5] J. Lee, F. Zhao, GWEC: Global Wind report 2022, 2022.

[6] V. Igwemezie, A. Mehmanparast, A. Kolios, Current trend in offshore wind energy sector and material requirements for fatigue resistance improvement in large wind turbine support structures – a review, Renewable and Sustainable Energy Reviews 101 (2019) 181–196.

[7] D. K. Sedlar, D. Vulin, G. Krajačić, L. Jukić, Offshore gas production infrastructure reutilisation for blue energy production, Renewable and Sustainable Energy Reviews 108 (2019) 159–174.

[8] P. Mendes, J. Correia, J. M. Castro, N. Fantuzzi, A. Aidibi, L. Manuel, Horizontal and vertical axis wind turbines on existing jacket platforms: Part 1 – A comparative study, Structures 32 (2021) 1069–1080. doi:10.1016/j.istruc.2021.01.069.

[9] D. Haselibozchaloee, J. Correia, P. Mendes, A. de Jesus, F. Berto, A review of fatigue damage assessment in offshore wind turbine support structure, International Journal of Fatigue (2022) 107145.

[10] S. Marquez, J. Sørensen, Fatigue reliability and calibration of fatigue design factors for offshore wind turbines, Energies 5 (2012) 2146–2147.

[11] T. Heo, D. P. Liu, L. Manuel, J. A. Correia, P. Mendes, Assessing fatigue damage in the reuse of a decommissioned offshore jacket platform to support a wind turbine, Journal of Offshore Mechanics and Arctic Engineering 145 (2023) 042002.

[12] J. Billingham, J. V. Sharp, J. . Spurrier, P. J. Kilgallon, Review of the performance of high strength steels used offshore, Review of the performance of high strength steels used offshore (2003).

[13] A. Necci, S. Tarantola, B. Vamanu, E. Krausmann, L. Ponte, Lessons learned from offshore oil and gas incidents in the arctic and other ice-prone seas, Ocean Engineering 185 (2019) 12–26. doi:https://doi.org/10.1016/j.oceaneng.2019.05.021.

[14] G. Liu, Y. Huang, K. Wu, J. Lan, Fatigue strength assessment of extra thick welded joints in offshore structures, The Nineteenth Interna-

tional Offshore and Polar Engineering Conference, Osaka, Japan (2009) ISOPE–I–09–200.

[15] K. L. Molski, P. Tarasiuk, Stress concentration factors for welded plate T-Joints subjected to tensile, bending and shearing loads, Materials 14 (2021) 546. doi:10.3390/ma14030546.

[16] D. Radaj, C. M. Sonsino, W. Fricke, Fatigue Assessment of Welded Joints by Local Approaches: Second Edition, 2006.

[17] J. Schijve, Fatigue predictions of welded joints and the effective notch stress concept, International Journal of Fatigue 45 (2012) 31–38.

[18] H. Xin, J. A. Correia, M. Veljkovic, F. Berto, L. Manuel, Residual stress effects on fatigue life prediction using hardness measurements for butt-welded joints made of high strength steels, International Journal of Fatigue 147 (2021).

[19] B. Vieira Ávila, J. Correia, H. Carvalho, N. Fantuzzi, A. De Jesus, F. Berto, Numerical analysis and discussion on the hot-spot stress concept applied to welded tubular KT joints, Engineering Failure Analysis 135 (2022) 106092. doi:10.1016/j.engfailanal.2022.106092.

[20] W. Cui, A state-of-the-art review on fatigue life prediction methods for metal structures, J. Mar. Sci. Technol. 7 (2002) 43–56. doi:10.1007/s007730200012.

[21] Z. Kala, Probabilistic modelling of fatigue crack-Some observations about conditional probability, Ph.D. thesis, KTH School of Engineering Sciences, Stockholm, Sweden, 2012.

[22] X.-P. Niu, R.-Z. Wang, D. Liao, S.-P. Zhu, X.-C. Zhang, B. Keshtegar, Probabilistic modeling of uncertainties in fatigue reliability analysis of turbine bladed disks, International Journal of Fatigue 142 (2021).

[23] J. Schijve, Statistical distribution functions and fatigue of structures, International Journal of Fatigue 27 (2005) 1031–1039.

[24] H. Jakubczak, W. Sobczykiewicz, G. Glinka, Fatigue reliability of structural components, International Journal Materials and Product Technology 25 (2006) 64–83. doi:10.1504/IJMPT.2006.008274.

[25] Committee on Fatigue and Fracture Reliability of the Committee on Structural Safety and Reliability of the Structural Division, Fatigue reliability: development of criteria for design', Journal of the Structural Division 108 (1982) 3–23. doi:10.1061/JSDEAG.0005869.

[26] P. H. Wirsching, Probabilistic Fatigue Analysis, Springer, Boston, MA, 1995, pp. 146–165. doi:10.1007/978-1-4615-1771-9_7.

[27] J. Barbosa, J. Correia, R. F. Júnior, S.-P. Zhu, A. M. D. Jesus, Probabilistic S-N fields based on statistical distributions applied to metallic and composite materials: State of the art, Advances in Mechanical Engineering 11 (2019). doi:10.1177/168781401987039.

[28] B. Pedrosa, J. Correia, C. A. S. Rebelo, M. Veljkovic, Reliability of fatigue strength curves for riveted connections using normal and weibull distribution functions, ASCE-ASME Journal of Risk and Uncertainty in Engineering Systems, Part A: Civil Engineering 6 (2020) 04020034.

[29] J. Correia, B. Pedrosa, P. Raposo, A. M. P. De Jesus, H. Gervásio, G. Lesiuk, C. Rebelo, R. Calçada, L. S. da Silva, Fatigue strength evaluation of resin-injected bolted connections using statistical analysis, Engineering 3 (2017) 795–805. Bridge Engineering and Tunnel Engineering.

[30] S. Hanaki, M. Yamashita, H. Uchida, M. Zako, On stochastic evaluation of S–N data based on fatigue strength distribution, International Journal of Fatigue 32 (2010) 605–609. Symposium on Competing Failure Modes and Variability in Fatigue.

[31] L. G. Mayorga, S. Sire, J. A. Correia, A. M. De Jesus, C. Rebelo, A. Fernández-Canteli, M. Ragueneau, B. Plu, Statistical evaluation of fatigue strength of double shear riveted connections and crack growth rates of materials from old bridges, Engineering Fracture Mechanics 185 (2017) 241–257.

[32] J. Correia, A. M. De Jesus, A. Silva, B. Pedrosa, C. Rebelo, R. Calçada, FE simulation of S-N curves for a riveted connection using two-stage fatigue models, Advances in Computational Design, an International Journal 2 (2017) 333–348. doi:10.12989/acd.2017.2.4.333.

[33] D. Leonetti, J. Maljaars, H. B. Snijder, Fatigue life prediction of hot-riveted shear connections using system reliability, Engineering Structures 186 (2019) 471–483.

[34] E. Castillo, A. Fernandez-Canteli, A Unified Statistical Methodology for Modeling Fatigue Damage, Springer Netherlands, 2009.

[35] A. Mohabeddine, J. Correia, P. Aires Montenegro, A. De Jesus, J. Castro, F. Berto, Probabilistic S-N curves for CFRP retrofitted steel details, International Journal of Fatigue 148 (2021) 106205. doi:10.1016/j.ijfatigue.2021.106205.

[36] E. Castillo, M. López-Aenlle, A. Ramos, A. Fernández-Canteli, R. Kieselbach, V. Esslinger, Specimen length effect on parameter estimation in modelling fatigue strength by Weibull distribution, International Journal of Fatigue 28 (2006) 1047–1058. Fatigue lifetime prediction of metals based on microstructural behaviour.

[37] A. Fernández Canteli, E. Castillo, S. Blasón, J. Correia, A. de Jesus, Generalization of the Weibull probabilistic compatible model to assess fatigue data into three domains: LCF, HCF and VHCF, International Journal of Fatigue 159 (2022). doi:10.1016/j.ijfatigue.2022.106771.

[38] J. Correia, P. Raposo, M. Muniz-Calvente, S. Blasón, G. Lesiuk, A. De Jesus, P. Moreira, R. Calçada, A. Canteli, A generalization of the fatigue Kohout-Věchet model for several fatigue damage parameters, Engineering Fracture Mechanics 185 (2017) 284–300. doi:10.1016/j.engfracmech.2017.06.009, XVIII International Colloquium Mechanical Fatigue of Metals.

[39] J. Schijve, Fatigue of Structures and Materials, 2 ed., Springer, New York, NY, 2009.

[40] R. Sakin, İrfan Ay, Statistical analysis of bending fatigue life data using

Weibull distribution in glass-fiber reinforced polyester composites, Materials & Design 29 (2008) 1170–1181. doi:10.1016/j.matdes.2007.05.005.

[41] J. A. Correia, A. M. De Jesus, A. Fernández-Canteli, Local unified probabilistic model for fatigue crack initiation and propagation: Application to a notched geometry, Engineering Structures 52 (2013) 394–407. doi:10.1016/j.engstruct.2013.03.009.

[42] P. Strzelecki, J. A. Correia, J. Sempruch, Estimation of fatigue S-N curves for aluminium based on tensile strength - proposed method, MATEC Web Conf. 338 (2021) 01026. doi:10.1051/matecconf/202133801026.

[43] D.-H. Kang, C. Jang, Y.-S. Park, S.-Y. Han, J. H. Kim, Fatigue reliability assessment of steel member using probabilistic stress-life method, International Journal of Fatigue 44 (2012) 128–137. doi:10.1155/2012/649215.

[44] P. D. Toasa Caiza, A. Ummenhofer, E. Castillo, E. Irassar, A probabilistic Stüssi function for modelling the S-N curves and its application on specimens made of steel S355J2+N, International Journal of Fatigue 132 (2020) 105779. doi:10.1016/j.ijfatigue.2018.07.041.

[45] J. Correia, A. Mourão, H. Xin, A. De Jesus, T. Bittencourt, R. Calçada, F. Berto, Fatigue strength assessment of riveted railway bridge details based on regression analyses combined with probabilistic models, Journal of Materials Research and Technology 23 (2023) 3257–3271. doi:10.1016/j.jmrt.2023.01.193.

[46] M. Guida, F. Penta, A Bayesian analysis of fatigue data, Structural Safety 32 (2010) 64–76. doi:10.1016/j.strusafe.2009.08.001.

[47] G. Edwards, L. Pacheco, A bayesian method for establishing fatigue design curves, Structural Safety 2 (1984) 27–38.

[48] Y. Chai, J. Peng, L. Xiao, X. Liu, J. Zhang, Fatigue Behavior of High-Performance Steel Beams Subjected to Different Corrosion Conditions, International Journal of Steel Structures 23 (2023) 1105–1118. doi:10.1007/s13296-023-00753-z.

[49] J. S. S. Sandviknes, N. D. Adasooriya, D. Pavlou, T. Hemmingsen, Environment-assisted fatigue of steel bridges: A conceptual framework for life assessment, IOP Conference Series: Materials Science and Engineering 1201 (2021) 012045. doi:10.1088/1757-899X/1201/1/012045.

[50] S. C. Siriwardane, N. D. Adasooriya, D. Pavlou, Fatigue strength curve for tubular joints of offshore structures under dynamic loading, Dynamics 1 (2021) 125–133. doi:10.3390/dynamics1010007.

[51] A. Milone, R. Landolfo, A Simplified Approach for the Corrosion Fatigue Assessment of Steel Structures in Aggressive Environments, Materials 15 (2022) 2210. doi:10.3390/ma15062210.

[52] N. D. Adasooriya, T. Hemmingsen, D. Pavlou, Fatigue strength degradation of metals in corrosive environments, IOP Conference Series: Materials Science and Engineering 276 (2017) 012039. doi:10.1088/1757-899X/276/1/012039.

[53] N. D. Adasooriya, D. Pavlou, T. Hemmingsen, Fatigue strength degradation of corroded structural details: A formula for S-N curve, Fatigue Fracture of Engineering Materials Structures 43 (2020) 721–733. doi:10.1111/ffe.13156.

[54] S. Suresh, Fatigue of Materials, 2 ed., Cambridge University Press, 1998.

[55] O. H. Basquin, The exponential law of endurance tests, 1961.

[56] Eurocode 3: Design of steel structures - Part 1-9: Fatigue, European Committee for Standardization, 2005.

[57] D. N. Veritas, DNVGL-RP-C203: Fatigue design of offshore steel structures, Høvik, 2011.

[58] J. Goodman, Mechanics Applied to Engineering, Nabu Press, Charleston, SC, USA, 2010.

[59] J. Morrow, Fatigue Properties of Metals, section 3.2, in: Fatigue Design Handbook, Soc. of Automotive Engineers, 1970.

[60] J. O. Smith, The effect of range of stress on the fatigue strength of metals, University of Illinois. Engineering Experiment Station. Bulletin; no. 334 (1942).

[61] N. E. Dowling, C. A. Calhoun, A. Arcari, Mean stress effects in stress-life fatigue and the walker equation, Fatigue & Fracture of Engineering Materials & Structures 32 (2009) 163–179.

[62] K. Walker, The Effect of Stress Ratio During Crack Propagation and Fatigue for 2024-T3 and 7075-T6 Aluminum, in: Effects of Environment

and Complex Load History on Fatigue Life, ASTM International, 1970. URL: https://doi.org/10.1520/STP32032S. doi:10.1520/STP32032S.

[63] R. Dantas, J. Correia, G. Lesiuk, D. Rozumek, S.-P. Zhu, A. de Jesus, L. Susmel, F. Berto, Evaluation of multiaxial high-cycle fatigue criteria under proportional loading for S355 steel, Engineering Failure Analysis 120 (2021) 105037. doi:10.1016/j.engfailanal.2020.105037.

[64] P. Mendes, M. Monteiro, J. A. Correia, M. Vieira, A. Reis, C. Horas, A. M. de Jesus, High-cycle rotating-bending fatigue performance of S690QL welded joints, Journal of Constructional Steel Research (2024). doi:10.1016/j.jcsr.2024.108488.

[65] I. O. for Standardization, ISO 18276: Welding consumables, Standard, International Institute of Standardization, 2017.

[66] P. H. Wirsching, J. T. P. Yao, Statistical Methods in Structural Fatigue, Journal of the Structural Division 96 (1970) 1201–1219. doi:10.1061/JSDEAG.0002603.

[67] R. J. Carroll, D. Ruppert, The Use and Misuse of Orthogonal Regression in Linear Errors-in-Variables Models, American Statistician 50 (1996) 1–6. doi:10.1080/00031305.1996.10473533.

[68] International Organization for Standardization, ISO 12107: Metallic materials — Fatigue testing — Statistical planning and analysis of data, Standard, International Institute of Standardization, 2012.

[69] American Society for Testing and Materials., ASTM E739-91 Standard Practice for Statistical Analysis of Linear Or Linearized Stress-life and

Strain-life Fatigue Data, Standard, American Society for Testing and Materials., 2004.

[70] A. Benard, E. C. Bos-Levenbach, The plotting of observations on probability paper (in Dutch) 7 (1955) 163–173.

[71] B. Wang, F. Islam, G. W. Mair, Evaluation methods for estimation of Weibull parameters used in Monte Carlo simulations for safety analysis of pressure vessels, Materials Testing 63 (2021) 379 – 385. doi:10.1515/mt-2020-0058.

[72] K. Störzel, J. Baumgartner, Statistical evaluation of fatigue tests using maximum likelihood, Materials Testing 63 (2021) 714–720. doi:10.1515/mt-2020-0116.

[73] J. I. McCool, Evaluating Weibull Endurance Data by the Method of Maximum Likelihood, ASLE Transactions (1970). doi:10.1080/05698197008972295.

[74] L. G. Rosa, I. Figueiredo, Demonstration of the robustness of maximum likelihood estimation to distinguish mixtures of two weibull populations in failure data of brittle materials, in: Advanced Materials Forum V, volume 636 of *Materials Science Forum*, Trans Tech Publications Ltd, 2010, pp. 1443–1450. doi:10.4028/www.scientific.net/MSF.636-637.1443.

[75] J. I. McCool, Using the Weibull Distribution: Reliability, Modeling, and Inference, Wiley, Chichester, England, UK, 2012.

[76] M. A. Nielsen, Parameter Estimation for the Two-Parameter Weibull Distribution, BYU ScholarsArchive (2011).

[77] R. C. S. Freire Júnior, A. S. Belísio, Probabilistic s–n curves using exponential and power laws equations, Composites Part B: Engineering 56 (2014) 582–590. doi:10.1016/j.compositesb.2013.08.036.

[78] J. A. Greenwood, J. M. Landwehr, N. C. Matalas, J. R. Wallis, Probability weighted moments: Definition and relation to parameters of several distributions expressable in inverse form, Water Resources Research 15 (1979) 1049–1054. doi:10.1029/WR015i005p01049.

[79] E. Castillo, A. S. Hadi, Parameter and quantile estimation for the generalized extreme-value distribution, Environmetrics 5 (1994) 417–432. doi:10.1002/env.3170050405.

[80] A. Fernández-Canteli, C. Przybilla, M. Nogal, M. L. Aenlle, E. Castillo, Profatigue: A software program for probabilistic assessment of experimental fatigue data sets, Procedia Engineering 74 (2014) 236–241. doi:10.1016/j.proeng.2014.06.255, XVII International Colloquium on Mechanical Fatigue of Metals (ICMFM17).

[81] X.-W. Liu, D.-G. Lu, P. C. Hoogenboom, Hierarchical bayesian fatigue data analysis, International Journal of Fatigue 100 (2017) 418–428.

[82] X.-W. Liu, D.-G. Lu, Survival analysis of fatigue data: Application of generalized linear models and hierarchical bayesian model, International Journal of Fatigue 117 (2018) 39–46. doi:10.1016/j.ijfatigue.2018.07.027.

[83] C. Z. Mooney, Monte Carlo simulation / Christopher Z. Mooney., Sage Publications, Thousand Oaks, California, 1997.

[84] J. R. Norris, Markov Chains, Cambridge Series in Statistical and Probabilistic Mathematics, Cambridge University Press, 1997. doi:10.1017/CBO9780511810633.

[85] W. K. Hastings, Monte Carlo sampling methods using Markov chains and their applications, Biometrika 57 (1970) 97–109. doi:10.1093/biomet/57.1.97.

[86] N. Metropolis, A. W. Rosenbluth, M. N. Rosenbluth, A. H. Teller, E. Teller, Equation of State Calculations by Fast Computing Machines, The journal of chemical physics 21 (1953) 1087–1092. doi:10.1063/1.1699114.

[87] L. David, J. Chris, B. Nicky, T. Andrew, S. David, The BUGS Book, Chapman & Hall, Boca Raton, FL, USA, 2012.

[88] E. Castillo, M. Muniz-Calvente, A. Fernández-Canteli, S. Blasón, Fatigue assessment strategy using bayesian techniques, Materials 12 (2019). URL: https://www.mdpi.com/1996-1944/12/19/3239. doi:10.3390/ma12193239.

[89] M. Li, W. Q. Meeker, Application of bayesian methods in reliability data analyses, Journal of Quality Technology 46 (2014) 1–23. URL: https://doi.org/10.1080/00224065.2014.11917951. doi:10.1080/00224065.2014.11917951. arXiv:https://doi.org/10.1080/00224065.2014.11

[90] A. F. Hobbacher, IIW document IIW-1823-07 recommendations for fatigue design of welded joints and components, International Institute of Welding (2008).

[91] H. E. Boyer, A. S. Metals, Atlas of Fatigue Curves, ASM International, 1985.

[92] A. J. McEvily, Atlas of Stress Corrosion and Corrosion Fatigue Curves, ASM International, 1990.

[93] T. Zhao, Z. Liu, C. Du, C. Dai, X. Li, B. Zhang, Corrosion fatigue crack initiation and initial propagation mechanism of E690 steel in simulated seawater, Materials Science and Engineering: A 708 (2017) 181–192. doi:10.1016/j.msea.2017.09.078.